AGU PUBLICATIONS

Neogene-Recent Reactivation of Pre-Existing Faults in South-Central Vietnam, with Implications for the Extrusion of Indochina

Nicholas Richard[1]*, Caroline M Burberry[1], Nguyen Hoang[2], Le Duc Anh[3], Sang Q Dinh[4], Lynne J Elkins[1]

[1] Department of Earth and Atmospheric Sciences, University of Nebraska-Lincoln, Lincoln, Nebraska.

[2] Institute of Geological Sciences, Vietnam Academy of Science and Technology (VAST), Hanoi, Vietnam.

[3] Institute of Marine Geology and Geophysics, VAST, Hanoi, Vietnam,

[4] South Vietnam Geological Mapping Division, Ho Chi Minh City, Vietnam.

* Nicholas Richard (nicholas.richard@huskers.unl.edu)

Key Points:

- In Vietnam, faults cross-cut basalt flows younger than ~0.6 Ma
- The orientation of faults and remotely sensed lineaments are related to a heterogeneous stress field in south-central Vietnam
- Five lithospheric microblocks in south-central Vietnam experienced a distinct tectonic history and are moving independently of each other

Abstract

Vietnam contains a complex series of faults coupled with a diffuse igneous province that has been active since the mid-Miocene. However, existing fault maps demonstrate little consensus over the location of Neogene basalt flows and relative ages of mapped faults, which complicates interpretations of tectonic model for the evolution of Indochina. This paper identifies discrete tectonic blocks within Vietnam and aims to define the Neogene-Recent tectonic setting and kinematics of south-central Vietnam by analyzing the orientation, kinematics, and relative ages of faults across each block. Fault ages and relative timing are constrained using cross-cutting relationships with dated basalt flows and between slickenside sets. Remote sensing results show distinct fault trends within individual blocks that are locally related to the orientations of the basement-involved block-bounding faults. Faults observed in the field indicate an early phase of dip-slip motion and a later phase of strike-slip motion, recording the rotation of blocks within a stress field. Faulting after the change in motion of the Red River Fault Zone is inferred, as faults cross-cut basalt flows as young as ~0.6 Ma. Strike-slip motion on block-bounding faults is consistent with rotation and continuous extrusion of each block within south-central Vietnam. The rotation of the blocks is attributed to the "continuum rubble" behavior of small crustal blocks influenced by extrusion-driven asthenospheric flow after the collision between India and Eurasia. We deduce a robust lithospheric-asthenospheric coupling in the extrusion model, which holds implications for other regions experiencing extrusion even in the absence of a free surface.

1. INTRODUCTION

The plate tectonic theory is a fundamental paradigm in the earth sciences, which has undergone modifications since its inception in the early 1960s; to accurately apply the plate tectonic framework to all settings, however, scientists must evaluate the most complex edge cases, such as collisional-adjacent regions like Indochina, Alaska, and Anatolia (Finzel et al., 2011; Redfield et al., 2007; Ridgeway & Flesch, 2007; Tapponnier et al., 1986). In such collisional settings, “extrusion” or “escape” tectonics is the process by which the collision of two tectonic terranes leads to the lateral escape of material formerly located between those terranes. Experimental studies have demonstrated that in addition to the impetus from an initial collision, the tectonic extrusion process also relies on a “free surface” for the escaping material to move toward (Tapponnier et al., 1982, 1986). For example, extrusion has been invoked to explain the tectonic motion and evolution of Alaska, where the free surface is the Bering Sea, and of the Anatolian block, where the free surface is the eastern Mediterranean, such that extrusion is

accommodated by extension in the Greek islands (Finzel et al., 2011; Redfield et al., 2007; Ridgeway & Flesch, 2007; Tapponnier et al., 1986). In detail, however, the mechanisms behind extrusion tectonics remain poorly constrained, including the mechanism for accommodating continuous extrusion if a free surface becomes unavailable by collisions (e.g., for Indochina, where the presence of Borneo marks the removal of a free surface; Figure 1) or by other tectonic processes (e.g., and also for Indochina, the presence of the southern reach of the East Vietnam Sea/South China Sea (EVS/SCS)). The topic of post-extrusion processes has been the subject of ongoing debate and remains an area of significant interest and scientific inquiry (Chen et al., 2017; Jolivet et al., 2018; Morley, 2002, 2016; Nguyen & Luong, 2019; Pubellier & Morley, 2014; Tapponnier et al., 1982, 1986; Taylor & Hayes, 1980). In this study, we thus aim to enhance our understanding of collision-adjacent tectonic deformation and extrusion tectonics exploring the consequences for extrusion following the removal of a free surface in Indochina.

We have selected south-central Vietnam, a part of the Indochina block, as our study area because of its location within the core of the larger Sundaland block (Figure 1), which has previously been described as experiencing homogeneous deformation as a rigid block with GPS-measured velocities between ~6 and ~10 mm/yr and an absolute motion to the ESE (e.g., Avouac & Tapponnier, 1993; Cardwell & Issacks, 1978; Curray, 1989; Fitch, 1972; Hall & Nichols, 2002; Hamilton, 1979; McCaffrey, 1991; Michel et al., 2001; Peltzer & Saucier, 1996; Simons et al., 2007; Tapponnier et al., 1982; Tran et al., 2013). In contrast, the stress field across the Sundaland block is heterogeneous rather than subparallel to the absolute motion vector (Nguyen & Luong, 2019; Tingay et al., 2010), suggesting that the question of whether this region can best be described in terms of block tectonics (Calais et al., 2006) or a continuous deformation field (Jade et al., 2004) is unresolved. In the case of Indochina, the block tectonics hypothesis of

Calais et al. (2006) is potentially compatible with an extrusion-driven origin for Neogene-Recent deformation in the region, while a continuous deformation field hypothesis, similar to deformation fields observed in regions like Tibet (Jade et al., 2004; Zhang et al., 2004), is more consistent with regional stretching and thermal subsidence related to EVS/SCS rifting.

This paper contributes to our understanding of post-extrusion tectonics by more thoroughly defining the Neogene-Recent tectonic setting, kinematics, and extrusion processes recorded in south-central Vietnam, using the orientations, slip senses and where possible, ages of faults. Together with regional fault maps (Kasatkin et al., 2017; Nguyen & Luong, 2019; the Geological and Mineral Resources Map of Vietnam, Gia Ray Region 1998; and B'Lao Region, 1998), our new data are then used to identify discrete tectonic microblocks within Vietnam, which are bounded by documented lithospheric-scale strike-slip faults, and to demonstrate that there has been Cenozoic fault activity in the Quang Nam, Kon Tum, Dray Sap North and South, Da Lat, and Tuy Hoa sectors of southern Vietnam that (1) post-dates volcanic activity in the diffuse igneous province; (2) potentially reactivates older faults; (3) is more consistent with an extrusion-based tectonic history than an extension-based tectonic history for the region; and (4) illustrates how extrusion may be accommodated once a free surface is no longer present. Our work expands upon previous work (e.g., Huchon et al., 1994; Nguyen & Luong, 2019; Rangin et al., 1995) as our lineament analysis covers a broader area, and our data sets, synthesis, and analysis allow us to reconcile conflicting information and models into a holistic tectonic model for south-central Vietnam.

2. GEOLOGIC SETTING

2.1 Stress Field Models

Extrusional and extensional tectonic models have previously both been invoked to characterize the complex stress field of Vietnam and Indochina (e.g., Simons et al., 2007; Tingay et al., 2010; Tran et al., 2013). One proposed model is that of "extrusion" or "escape" tectonics, the process by which the collision of two tectonic terranes leads to escape of material formerly located between those terranes, after Tapponnier et al. (1982, 1986). The proposed extrusion model for Indochina (e.g., Chamot-Rooke & Le Pichon, 1999; Chi & Dorobek, 2004; Chi & Geissman, 2013; Flower et al., 1998; Hoang & Flower, 1998; Michel et al., 2001; Morley, 2007; Tingay et al., 2010; Yan et al., 2006) posits that (1) strong coupling between the asthenosphere and lithosphere and a significant mantle drag torque has translated the Southern Indochina microplate, in response to extrusion of asthenosphere by the closure of the Tethys Sea and Himalayan collision; and (2) the extruded lithospheric block is characterized by a combination of giant strike-slip faults, smaller scale strike-slip faults and pull-apart basins, and minor normal faulting. Alternatively, an extensional model has been suggested based on seismic interpretation from two basins offshore from southern Vietnam, which exhibit a phase of rifting coeval with the propagation of the EVS/SCS rift zone, ascribing the presence of more recent faulting and diffuse continental volcanic activity purely to the westward propagation of this rift and associated thermal subsidence (Figure 1; Fyhn et al., 2009a, b). These basinal data suggest that normal faulting off-shore predates the voluminous, subaerial volcanism, and that the subsequent volcanic flows erupted into existing rift or pull-apart basins (Huchon et al., 1994). However, newer age constraints indicate that EVS/SCS spreading ceased at ~16 Ma (Li et al., 2015), and it is unclear whether far-field thermal subsidence can induce fault activity in this manner.

2.2. Extrusion Tectonics

123 The Red River Fault Zone in northern Vietnam, along with the Wang Chao Fault Zone
124 (WCFZ) and Three Pagoda Shear Zone (TPSZ), have been described as sinistral shear zones
125 related to the extrusion of Indochina during the Cenozoic (Figure 1; Jolivet et al., 1999; Lacassin
126 et al., 1997; Rangin et al., 1995). As noted above, here "extrusion" of Indochina refers to the
127 modification of structures and geodynamics of Indochina following the India-Asia hard collision,
128 which resulted in the lateral migration and clockwise rotation of Indochina (Hall, 2002; Hu et al.,
129 2015; Michel et al., 2001; Richter & Fuller, 1996; Simons et al., 2007; Tapponnier et al., 1982;
130 Zhao et al., 2016). The hard collision between India and Asia led to the thickening of the
131 continental crust of the Tibetan Plateau, causing upper mantle flow to migrate towards the
132 thinned Southeast Asian lithosphere to the southeast (Jolivet et al., 2018). The extrusion model
133 for Indochina assumes a component of mantle flow roughly parallel to the strike of the major
134 strike-slip faults (e.g., Flower et al., 1998; Hoang and Flower, 1998; Yan et al., 2006), which is
135 corroborated by anisotropy recorded in shear-wave splitting data for the upper mantle beneath
136 the northern part of the Indochina-Shan Tai complex (Bai et al., 2009). One major challenge to
137 the extrusion model, however, is that sinistral motion along the RRFZ ceased at ~17 Ma and
138 became dextral by ~5.5 Ma (e.g., Fyhn & Phach, 2015; Leloup et al., 1995, 2001; Zhu et al.,
139 2009). Cessation of sinistral movement has been considered to mark the end of extrusion of the
140 Indochina block (Leloup et al., 1995, 2001; Zhu et al., 2009) but may instead mark a change in
141 regional or local kinematics. The cause of this regional change in plate kinematics is variously
142 ascribed to the ~23.6 Ma ridge jump in the EVS/SCS (Li et al., 2015), a change in Indian
143 indentor motion (i.e., coupling of the Indian and Burmese blocks (Fyhn et al., 2009a, 2009b), or
144 an additional plate tectonic reconfiguration in the region such as the collision of Australian
145 fragments to the SE of Sundaland (Pubellier & Morley, 2014).

2.3. Extensional Tectonics

Two major back-arc basins existed in Vietnam during the Permian and Jurassic-Cretaceous periods (Ferrari et al., 2008; Hall, 1996, 2012; Hara et al., 2018; Metcalfe, 2013a, 2017; Morley, 2012; Waight et al., 2021). The E-NE directed subduction of the Paleo-Tethys Ocean during the Permian led to the formation of the Sukhothai-Chanthaburi Volcanic Arc, located on the western edge of Indochina (Metcalfe, 2017; Waight et al., 2021). The Nan-Uttaradit and Sa-Kaeo sutures, situated in Southeast Asia, have been suggested to mark the boundary between Indochina and the Sukhothai Terrane, belived to be the site of a remnant Permian back-arc basin (Hara et al., 2018; Metcalfe, 2017; Sone and Metcalfe, 2008; Sone et al., 2012 Wang et al., 2018). Tri and Khuc (2011), through a remote sensing and field-based study, suggested that during the Early and Middle Jurassic, Southern Vietnam was situated in a passive margin setting along the eastern edge of the Indochina plate. This passive margin setting transitioned into a more dynamic back-arc fold-thrust belt, marked by a shift from passive to active tectonic setting, with subsequent deformation driven by changes in subduction angle and/or subduction obliquity during the Jurassic (Schmidt et al. 2021). Throughout the Late Jurassic and the Cretaceous, igneous activity along the coastlines of southern Vietnam and southeastern China was linked to an eastern subduction zone (Thuy et al., 2004; Shellnutt et al., 2013; Xu et al., 2016; Schmidt et al., 2021). During this time a, NW-SE oriented back-arc formed in south-central Vietnam (Ferrari et al., 2008; Hall, 1996, 2012; Hara et al., 2018; Metcalfe, 2013a, 2017; Morley, 2012; Waight et al., 2021).

During the Late Cretaceous, rifting initiated within the proto-South China Sea basin, giving rise to an ENE-WSW-oriented extensional fault system (Barckhausen et al., 2014; Chung et al., 1997; Ye et al., 2018; Zhou et al., 1995). Rifting of the Proto-South China Sea was followed by

the opening of the NE-SW striking EVS/SCS proper at ~32 Ma. (Briais et al., 1993; Carter et al., 2000; Chung et al., 1997; Clift et al., 2008; Zhou et al., 1993). Spreading subsequently either ceased at ~20.5 Ma (Barckhausen et al., 2014) or ~16 Ma in the southwest sub-basin of the EVS/SCS, closest to our study area (Li et al., 2015). After EVS/SCS spreading ceased, some studies have proposed that rifting may have propagated westward into continental Vietnam, while lingering upper mantle upwelling generated ongoing diffuse seamount activity within the EVS/SCS (Barckhausen et al., 2014; Cullen et al., 2010; Matthews et al., 1997; Yan et al., 2006). The 16 Ma age of Li et al. (2015) also approximately corresponds with the cessation of sinistral motion along the Red River Fault Zone (RRFZ; Figure 1), marking a simultaneous change in regional plate kinematics.

2.3. Identification of Regional Lithospheric Sectors

Kasatkin et al. (2017) mapped a series of large-scale strike-slip faults that divide the study area into discrete lithospheric sectors with distinct basement lithologies (Figure 2). The northernmost sector, the Quang Nam sector, consists of a Precambrian to Paleozoic accretionary belt (Anh et al., 2021; Tung & Tri, 1992) bounded by the Tam-Ky Phuoc Son Shear Zone (TKPSSZ) to the south and the East Vietnam Transfer Zone (EVTZ) to the east. A major Mesozoic suture zone was likely present along what are presently the TKPSSZ and the Poko Shear Zone (PKSZ), inferred from (1) continuity of kinematic indicators and deformation, (2) allochthonous assemblages of ophiolitic mafic to ultramafic rocks; (3) highly deformed migmatites; and (4) arc-type volcanic lithologies (Lepvrier et al., 1997, 2004, 2008; Tran et al., 2014; Van et al., 2001). The EVTZ is a large-scale transform fault inferred to be a regional, extrusion-related fault and is linked to the RRFZ (Fyhn & Phach, 2015; Fyhn et al., 2018; Leloup

et al., 2001; Nguyen et al., 2012; Phach & Anh, 2018; Tapponnier et al., 1986). Several models have proposed that the EVTZ serves as the eastern boundary of the Indosinian block, and the transtensional sinistral slip along the EVTZ has been identified by some authors as the primary driving force for the opening of the EVS/SCS (Hall, 2002; Leloup et al., 1995, 2001; Tapponnier et al., 1986).

The geographically central sector in Vietnam is widely known as the Kon Tum Massif (Figure 2; Jiang et al., 2020; Katz, 1993; Lan et al., 2003; Lepvrier et al., 2004; Nagy et al., 2001; Nam et al., 2001). Previous studies have inferred an Archean age for Kon Tum Massif basement based on petrogenic similarities to other Archean Gondwana-derived terranes in India, Australia, Sri Lanka, and East Antarctica (Hutchison, 1989; Katz, 1993). Sparse data (e.g., Hf model ages from inherited zircons in granites) instead suggest a Paleoproterozoic age for some of the basement in this region (Hung et al., 2022). However, U-Pb ages from basement granulites, migmatites, gneisses, and schists are considerably younger and Permo-Triassic to early Paleozoic in age (Jiang et al., 2020; Lan et al., 2003; Lepvrier et al., 2004; Nagy et al., 2001; Roger et al., 2007; Usuki et al., 2009). The EVTZ (east), PKSZ (west), TKPSSZ (north), and the Song Ba Fault (SBF; south) bound the Kon Tum Massif (Figure 2). The SBF is a deep-seated, strike-slip fault that extends for >300 km along the southern and western edge of the Massif (Nielsen et al., 2007; Figure 2), and connects to the Tuy Hoa shear zone and parallels extrusion-related strike-slip faults such as the RRFZ, WCFZ, and the TPSZ (Figure 1; Than et al. 2003; Zhang et al., 2011).

Mesozoic and Paleozoic accretionary terranes compose the basement of the two southernmost lithosphere sectors, Da Lat and Dray Sap (Figure 2; Anh et al., 2021; Tung & Tri, 1991). The Tuy Hoa-Cu Chi Fault (THCCF) separates the two southern lithosphere sectors

(Nguyen & Luong, 2019) and is a prominent fault system believed to have originated during the Eocene-Miocene, following the Cenozoic extrusion of the Indochina block (Phach & Anh, 2018).

In summary, the basement ages of each lithospheric sector fall either within the Permian and Jurassic-Cretaceous Indosinian orogeny or within a preceding thermotactic event (Waight et al., 2021). The bounding faults themselves are either ancient suture zones or are long-lived, large-scale, lithospheric, extrusion-related faults (Kasatkin et al., 2017; Lepvrier et al., 2004, 2008; Nguyen & Luong, 2019; Phach & Anh, 2018; Tran et al., 2014; Van et al., 2001).

3. METHODS

This is a combined remote-sensing and field-based study. We interpreted lineaments across the field area using Landsat ETM+ data and DEM data. Landsat ETM+ and DEM datasets were sourced from the Global Land Cover Facility and the Open Development Mekong website respectively. Landsat ETM+ data were downloaded as separate bands and combined into a false-color composite; specifically, bands 531 were combined as RGB in ArcGIS, and this raster was stretched using the histogram equalize operation. Landsat ETM+ data were also combined as a true color composite using bands 321 as RGB in ArcGIS. Datasets were already referenced to a WGS84 reference frame, so no conversions were necessary. The remote datasets were compiled into an ArcGIS project, and other information was incorporated by database upload or by georeferencing JPG files. Other information comprises: (1) our own field locations; (2) lineament maps from Huchon et al. (1994), Nguyen & Luong (2019), Rangin et al. (1995; Figure 3), and a series of Geological and Mineral Resources Maps (Department of Geology and

Minerals, Vietnam, 1998); and 3) locations with dated basalt samples from An et al. (2017), Hoang et al. (2019), and Lee et al. (1998).

Following the methods of Drury (2004), lineaments were picked from the remote datasets based on textural changes in the images and DEM (Table 1). Linear changes in the texture of the land surface often indicate a fault-controlled change, although care must be taken to avoid regions where human activity has altered the land surface**;** such regions can be identified by the typical regular checkerboard pattern of cultivated fields and field boundaries and the proximity to dwellings. However, at the scale used (1:300,000, selected for ease of comparison to recent maps from Nguyen & Luong (2019)) the checkerboard pattern of human cultivation cannot be discerned in the DEM images. We were typically unable to ground-truth the lineament mapping in the field because of the variation in scale between mapped lineaments (typically 10s of km long) and field-scale observations.

Table 1
Sector name, key lineament orientations.

Sector name/dataset name	**Key lineament orientations with corresponding s/s faults (*italics*)**
Tuy Hoa Sector	NW-SE (*SBF*), NE-SW (*THCCF, EVTZ*)
Da Lat Sector	NW-SE (*SBF*), NE-SW (*THCCF, VTCNF*)
Quang Nam Sector	N, NE-SW (*EVTZ*), E-W (*TKPSSZ*)
Kon Tum Sector	N-S (*EVTZ, PKSZ*), NE-SW (*THCCF*)
Dray Sap Sector (N)	N-S (*PKSZ*), NE-SW (*THCCF*), NW-SE (*SBF*)
Dray Sap Sector (S)	N-S (*PKSZ*), NE-SW (*THCCF*), E-W, NW-SE (*SBF*)
Huchon et al. (1994)	N-S, NW-SE, NE-SW
Nguyen & Luong (2019)	N-S NW-SE, NE-SW

Rangin et al. (1995)	N-S, NW-SE, NE-SW

The three regional datasets in the last three rows do not include strike-slip fault information
Fault names for abbreviations are given in Figure 2.

We undertook three field trips to the region in 2016, 2018, and 2020 (Figure 2). The first was a reconnaissance expedition in 2016 to the southern part of the Central Highlands, near Ho Chi Minh City, Buon Ma Thuot, and Vung Tau. The second was a more extended expedition aimed at observing the structural geology in the Central Highlands. For the final field season, we focused on fault slip sense and targeted key locations not previously visited in the Quang Nam, Kon Tum, and Da Lat sectors (Table S1). We observed lithology at every stop, and where relevant, we made measurements of bedding attitude, fault attitude, slickenside pitch within the fault plane, and where possible, fault kinematics or apparent offset, where true slip sense could not be determined. At each site, we documented any cross-cutting relationships between faults and the host lithology, considering whether the fault terminated against lithological elements or cut all observable lithologies. In some locations, the relationships between different generations of slickensides were observed and noted. On our return to the lab, these data were synthesized using GIS, Stereonet 10™, and FaultKin™ (Allmendinger et al., 2012; Marrett & Allmendinger, 1990) to determine relationships to the lineament map, similarity in fault orientations, and analysis of stress regimes, respectively.

To bracket the age of faulting, the age of an alkali basalt flow (field sample number 2016-CH-10; ISGN: 10.58052/IEVNR000R), retrieved from location 11 (10.5076ºN, 107.2729ºE, and ~70 m ft. elevation) was determined using $^{40}Ar/^{39}Ar$ methods at the Oregon State University Argon Geochronology Lab in Corvallis, Oregon. This sample was used in conjunction with existing lava flow and core dates from basalt plateaus from An et al. (2017), Hoang et al. (2019), and Lee et al. (1998). The sample was crushed, sieved to ~300 μm grain size, rinsed in distilled water, dried at low temperature in an oven at ~80ºC, then mildly leached to remove impurities.

The procedure for leaching was a 20-minute soak in 5% HNO_3 in an ultrasonic bath, followed by 3 rinses in distilled water, then a 20-minute soak in distilled water in the ultrasonic bath and 3 more distilled water rinses; the sample was then again dried at 80ºC or lower in the oven. The sample was then irradiated in the TRIGA experimental reactor at the OSU Radiation Center at 1 MW power. The neutron flux during irradiation was monitored using the FCT-NM standard, with an adopted age of 28.20 ± 0.02 Ma (after Kuiper et al., 2008), $^{40}Ar/^{39}Ar$ = 9.733 ± 0.008, and J-value of 0.001615 ± 0.000001. For mass spectrometry, the sample was analyzed by incremental heating using a bulk CO_2 laser heating method on the ARGUS-VI-D instrument at OSU. Ages were determined using a decay constant of 5.53 ± 0.05 x 10^{-10} a^{-1} (Steiger & Jäger, 1977) and age correction methods after Min et al. (2000). Heating plateau ages were determined using an error-weighted mean of plateau steps. Additional standard and procedural blank results are available in Burberry et al. (2023).

4. RESULTS

4.1. Results from remote sensing data

The DEM dataset is presented in Figure 4, overlain on a hillshade dataset for ease of visualization. The figure also includes field locations, notable strike-slip faults, and the identified lineaments from this study. Figure 5a-f shows rose diagrams for our measured lineament orientations within each sector bounded by the major strike-slip faults, using the fault boundaries identified by Kasatkin et al. (2017). For comparison, Figure 5 also includes rose diagrams of lineaments from other studies conducted by Huchon et al. (1994) (Figure 5g), Nguyen & Luong (2019) (Figure 5i), and Rangin et al. (1995) (Figure 5h), and as shown in Figure 3. The red bars

in Figure 5 show the dominant strikes of the EVTZ, SBF, THCCF, TKPSSZ, and VTCNF fault zones.

Despite the discrepancy in the number of lineaments in each rose diagram, some patterns emerge with lineaments having orientations consistent with adjacent large-scale strike-slip faults (Figures 4, 5, Table 1). Lineaments from our study (Figures 4, 5a-f) overall exhibit orientations consistent with the adjacent large-scale strike-slip faults mapped by Kasatkin et al (2017) that bound each sector. Lineaments from other published studies (Huchon et al., 1994; Nguyen & Luong, 2019; Rangin et al., 1995; Figures 3, 4, Table 1) overall exhibit three prominent orientations, N-S, NW-SE and NE-SW. The results of these three studies are also consistent with our data and the adjacent large-scale strike-slip faults.

4.2. Fault orientations from field data

Figure 6 shows the fault plane orientations measured in the field, grouped by lithospheric sector (after Figure 2, Table 1). Table S1 presents geographic coordinates, sector names, brief outcrop descriptions, pertinent measurement information, and prominent fault orientations for all reported field sites. We measured a total of 349 fault attitudes at 26 field localities. Using this data set, we then inferred an overall, dominant fault trend for each locality, illustrated by red lines in Figure 6a.

We observe that the orientations of the dominant faults for each lithospheric sector are distinct from one another. In all sectors, fault orientations are similar to adjacent large-scale strike-slip faults and other regional fault systems, as outlined in Table 2. In the Tuy Hoa sector, fault orientations are similar to those of the adjacent SBF and THCCF. Similarly, faults in the Da Lat sector are subparallel to the adjacent strike-slip faults mapped by Kasatkin et al. (2017;

VTCNF, THCCF, and SBF), along with the EVTZ. The dominant fault attitudes in the Quang Nam sector mimic the EVTZ, with some resembling the TKPSSZ. The Kon Tum and Dray Sap sectors exhibit fault patterns similar to the previously mentioned sectors in that they likewise mirror the adjacent strike-slip faults (Kasatkin et al., 2017).

4.3. Analysis of faulting regimes

The results from moment tensor solutions in FaultKin™, using slickenside data from the observed fault planes, are depicted in Figure 7, and Figure 8 illustrates the orientations of tensional axes calculated from FaultKin™, all for moment tensor solutions categorized as younger, older, and undefined based on observed field relationships. “Oldest” and “youngest” sets of slickensides were defined where we observed clearly visible cross-cutting relationships in outcrop. We categorized all other slickenside data without visible cross-cutting relationships, or where we could not bracket fault movement age independently, as “undefined.” Overall, older orientations produced solutions with a dominantly normal (to slightly oblique) sense of motion, while younger faults have an oblique (to strike-slip) sense of motion.

We developed moment tensor solutions for the Da Lat, Tuy Hoa, and Dray Sap sectors from seven locations (Figure 7, and locations 1, 4, 6, 14, 15, 23, and 26). Based on cross-cutting slickensides observed in the field (such as the examples shown in Figure 9), the moment tensor solutions (Figure 7), and the trends and plunges of tensional stress axes (Figure 8), there appears to be a heterogeneous stress field that has changed with time. In the Da Lat and Tuy Hoa sectors, older solutions have a normal to oblique-slip sense, while younger solutions have a strike-slip to oblique-slip-sense, regardless of fault orientation. In both Dray Sap sectors, we also have “undefined” strike-slip-like moment tensor solutions at locations 23 and 26 (Figure 7).

For the Kon Tum and Quang Nam sectors, our moment tensor solutions indicate a heterogeneous stress field similar to that of the Tuy Hoa, Da Lat and Dray Sap sectors (Figure 7). In the Kon Tum and Quang Nam sectors we have five moment tensor solutions (locations 16, 18, 19, 21 and 22). We were able to define younger and older sets of slickensides at locations 18 and 21, while slickensides at locations 16, 21 and 22 are undefined (Figure 7). From our solutions combined with pitch angles measured in the field (Figure 9), we observe that similar to Tuy Hoa, Da Lat and Dray Sap, the younger fault motion set in Kon Tum and Quang Nam has a strike-slip to oblique-slip sense, while the older motion has a dip-slip to oblique-slip sense. At locations 16, 19 and 22, our additional slickenside measurements, whose relative ages are "undefined," exhibit moment tensor solutions with a strike-slip to slightly oblique-slip sense.

4.4. Absolute Ages

The field photograph in Figure 10a for map location 14 shows the presence of closely spaced NE-SW striking faults that intersect the Pliocene Soc Lu Formation, indicating a fault age younger than Pliocene. Additional field photographs in Figures 10b and c show apparent offset of Cenozoic intrusions and lava flows cross-cut by fault planes. To achieve more quantitative age constraints in this study's field area, we measured an additional $^{40}Ar/^{39}Ar$ age of 0.6 ± 0.004 Ma in basalt sample 2016-CH-10 (ISGN: 10.58052/IEVNR000R) from location 11 (Figure 11; see Supplementary Information). For additional regional age constraints, Figure 11 presents a more detailed geologic map depicting part of the Da Lat sector with sample sites of interest. From the cross-cutting lineaments on the map intersecting multiple dated basalt flows, it can be inferred that the fault ages are younger than ~0.6 Ma, based on our Ar-age data and those reported by Lee et al. (1998).

5. DISCUSSION

5.1. Tectonic Microblocks of South-Central Vietnam

Given that fault orientations are distinct in each sector (Figure 6a), we interpret the varying lineament and fault trends within each fault population to indicate that the Da Lat, Dray Sap, Kon Tum, Quang Nam and Tuy Hoa sectors are tectonically discrete microblocks. From here on, we will use the word “microblock” to describe the geographical sectors described above. We further infer that the lithospheric-scale strike-slip faults mapped by Kasatkin et al. (2017) bound the five discrete tectonic microblocks (Figure 2). Lastly, based on sharp changes in fault and lineament orientations in the Dray Sap microblock (Figure 4), namely a change from dominantly E-w lineaments in the south to dominantly N-S lineaments in the north, we further postulate the presence of a previously unmapped fault (shown as a dashed line in Figures 2, 4 and 7), which divides the Dray Sap microblock into northern and southern sections. As further justification for our microblock model, we note that each lithospheric sector or microblock contains a distinct basement lithology and has a distinct geologic history (Sections 2.2 and 2.3), and each is bounded by deep-seated oblique-slip faults or Mesozoic suture zones. The stress regime solutions shown in Figure 7 are likewise distinct in each microblock.

5.2 Tectonic History of South-Central Vietnam

5.1.2. Evolution of Vietnam Microblocks

As described above, cross-cutting slickensides in several field locations, along with the trend and plunge of tensional axes (Figure 8), provide additional insights into changes in stress fields over time within each microblock. Figures 7, 8 and 9 imply that there was an early phase of dip-slip on many faults, followed by oblique- to strike-slip motion. We infer from cross-cutting

slickensides that the Kon Tum, Tuy Hoa and Da Lat microblocks initially hosted dip-slip, likely normal faults (Figure 9). Unfortunately, we were unable to confirm a similar history for the Quang Nam and Dray Sap microblocks based on our data set.

We lack timing constraints on the ages of the fault sets defined as “older” in this study, which can be found to cut Jurassic sediments (e.g. Location 15) and are, therefore, only constrained as definitively younger than Jurassic rocks. Furthermore, while the moment tensor solution calculated for Location 15 aligns with the strike orientation delineated by Rangin et al. (1995; Figure 3c), it does not match the prevailing fault trend observed in the region (Figures 6, 7). We believe this discrepancy suggests that the principal stress indicated by the older moment tensor solution is likely related to a significantly earlier tectonic event, likely Jurassic, and that this fault likely persists in the subsurface. Overall, we postulate that the “older”, dip-slip episode is related to back-arc rifting during the Jurassic-Cretaceous. Support for this interpretation comes from our cross-cutting age relationships and the co-alignment of fault and moment tensor solution orientations to local Jurassic-Cretaceous extensional tectonics (Hall, 1996; Morley, 2012; Nam, 1995) (Figure 8).

Figures 7, 8 9, and 10 together imply that there was a recent phase of oblique- to strike-slip motion on many faults in our study area. Based on published basalt ages (Hoang et al., 2013, 2019; Lee et al., 1998), our $^{40}Ar/^{39}Ar$ dates, and the cross-cutting slickensides observed in the field (Figures 10, 11), we postulate that the more recent oblique to strike-slip motion was active until at least ~0.6 Ma. The more recent activity associated with oblique- to strike-slip motion, in contrast to the older dip-slip type of faulting, exhibitis significant heterogeneity in the moment tensor solutions across the field area (Figures 7, 8). For example, based on relationships in Figure 7 and 8, the differences in young moment tensor solutions between map locations 1 in the Tuy

Hoa microblocks, locations 4, 6 and 15 in the Da Lat microblock, and locations 1, 18 and 21 in the Kon Tum microblock suggest that these microblocks are experiencing internal deformation independent of one another. This young, heterogeneous stress field, characterized by oblique- to strike-slip moment tensor solutions, is indicative of an extrusion tectonic regime rather than an extensional one, which would exhibit more homogeneity and predominantly dip-slip faults in the moment tensor solutions.

5.2. Continuum Rubble Tectonic Model for Indochina

As described by Dewey et al. (2008) for the Coso region of Southern California, we posit that some of the microblocks of south-central Vietnam are undergoing rotation about vertical axes, as well as potential internal deformation in a broadly transtensional regime. Dewey et al. (2008) described this working model as the "continuum rubble" behavior of small blocks, and we find this term valuable to describe the rotation and "jostling" of the microblocks of Indochina between the Ailo Shan-Red River Fault Zone and the Mae Ping Fault Zone (Figure 1). Numerical models for the Coso region, e.g., by Eckert & Connolly (2007) and Pearce & Dewey (2008) show that both dip-slip and wrench faulting components can be found in such a "continuum rubble" regime, together with the development of significant breakup of a large lithospheric block into what Eckert and Connolly (2007) call "second-order" fractures. These models further support our suggestion that such continuum rubble behavior can explain the polyphase deformation observed on the faults in south-central Vietnam, with both dip-slip and wrench-faulting components.

5.3. Continuous Extrusion of Microblocks

Contrary to existing literature (e.g., Rangin et al., 1995; Searle et al., 2010; Zhu et al., 2009), which suggests that faulting associated with both extrusion and extensional tectonic regimes has ceased in the Indochina Peninsula, our results (e.g., Figure 11) demonstrate that faulting has been more recent than lava flows dated 4.3 ± 0.2 Ma (An et al. 2017), 0.6 ± 0.004 Ma (this study), and 0.24 ± 0.1 Ma (Lee et al., 1998). These age constraints indicate that some faulting is significantly more recent than the last two documented major pulses of basaltic volcanism (5.4-1.75 Ma and 0.7-0.57 Ma; Tri et al., 2011), than the postulated end of tectonic extrusion based on the change in motion of the Red River Fault Zone (5.5 Ma; Leloup et al., 1995, 2001; Zhu et al., 2009) and, significantly, than the cessation of rifting in the EVS/SCS (~16 Ma; Li et al., 2015). Thus, a tectonic regime more complex than thermal subsidence must be operating across Vietnam. Given our evidence for a highly heterogeneous stress field and our inferred fault ages, we propose that the relatively recent fault slip motions within the study area can instead be attributed to ongoing extrusion tectonics.

As mentioned, paleomagnetic and GPS data from the core of the Sundaland block show that the Kon Tum microblock is likely moving to the east and rotating clockwise within Sundaland (Chamot-Rooke and Le Pichon, 1999; Chi and Dorobek, 2004; Chi and Geissman, 2013; Cung and Geissman, 2013; Michel et al., 2001; Morley, 2007; Tingay et al., 2010; Tran et al., 2013). This rotation is consistent with a regional model whereby Sundaland is composed of not a rigid core, but a continuum rubble of fragments that interact, internally deform, and in some cases rotate about vertical axes with respect to one another under regional stresses. The eastward motion of the Kon Tum microblock is thus consistent with the continued extrusion of material from the Himalayan collision to the east and southeast. The Da Lat, Tuy Hoa, and Quang Nam microblocks lack GPS data at a fine enough scale to resolve the proposed motion and merit

464 further investigation (Nguyen & Luong, 2019, and references therein), but we posit that they are
465 responding to similar regional tectonic processes.

466 The Red River Fault Zone ceased sinistral motion ~17 Ma and initiated dextral motion ~5.5
467 Ma (e.g., Leloup et al., 1995, 2001; Zhu et al., 2009; Zuchiewicz et al., 2013). As noted above,
468 the 17 Ma change was previously inferred to mark the end of extrusion in Indochina. However,
469 instead, we suggest that this event marks a change in the kinematics of the extrusion process. The
470 postulated end of tectonic extrusion does not account for the asthenospheric flow associated with
471 the extrusion of Indochina, or for documented ongoing volcanism (e.g., the 1923 eruption of Île
472 des Cendres), which instead suggest continued mantle flow. To accommodate the motion of
473 mantle flow beneath the Shan Tai, Kon Tum, Da Lat, and other microblocks would require
474 rotation of those blocks within the confines of the larger-scale shear zone defined by the Red-
475 River–East Vietnam Transform and Mae Ping Fault Zones. This rotation is required because
476 there is no free surface into which these blocks can be extruded, given their position in the core
477 region of Sundaland and the presence of Borneo.

478
479 **6. CONCLUSIONS**
480

481 To characterize controls on present-day deformation in south-central Vietnam, we measured fault
482 data throughout the region, which we compared to remote sensing data from this and previous
483 studies (Huchon et al., 1994a; Nguyen & Luong, 2019; Rangin et al., 1995). We also compared
484 the cross-cutting relationships between various observed and measured slickensides to infer the
485 change in fault slip over time, and the relationships of faults with basalt flows of a given age to
486 constrain the age of faulting throughout the study area. We conclude that: (1) cross-cutting
487 relationships between faults and basalt flows support recent faulting within Vietnam; (2) fault
488 and lineament orientations suggest a locally heterogeneous stress field related to the faults

mapped by Kasatkin et al. (2017); (3) dip- to oblique-slip faults were reactivated during the extrusion of Indochina; (4) recent strike- to oblique-slip faults and stress fields suggest continuous extrusion of Indochina; and (5) each lithospheric sector (or microblock) has a different tectonic history and moves independently. Finally, the breakup of Indochina into these microblocks is likely to have occurred at the same time as the cessation of spreading in the EVS/SCS and the change in motion on the RRFZ at ~17 Ma, which was previously suggested to indicate the end of local tectonic extrusion. Instead, we postulate that these changes indicate a change in the kinematics of the extrusion process, as extrusion continues in the absence of a free surface. We suggest that once the free surface is removed by other tectonic processes, block breakup and rotation are the inevitable consequence of ongoing mantle flow and that for extrusion to occur, a strong lithospheric-asthenospheric coupling is, in fact, necessary.

Acknowledgments

The Authors acknowledge a University of Nebraska-Lincoln College of Arts and Sciences International Partnerships Grant and NSF Grant EAR-1758972. We also acknowledge the OSU Argon Geochronology Lab, particularly Dan Miggins, who made the measurements on the sample referenced in this paper. Remote sensing data were purchased from Apollo Mapping$^{TM?}$. Figure 11 was created using the remote sensing data and Department of Geology and Minerals maps of the Gia Ray and B'Lao regions by Nathan Sorsen for an undergraduate research project. We gratefully acknowledge the sterling contributions of John Lassiter, Kirby Hobbs, Tran T. Huong, Nguyen T. Mai and Ipsita Mitra.

Open Research

There is a Mendeley Dataset (Burberry et al., 2023), which has the reserved DOI of 10.17632/h4v7srkpc2.2. This dataset contains all structural measurements from the three field campaigns (2016, 2018 and 2020), the full

lineament dataset as orientations, and the Ar-Ar data. It is an updated version of a previous dataset which did not contain the full lineament dataset or the full structural dataset.

References

Allmendinger, R. W., Cardozo, N. C., & Fisher, D. (2012). *Structural Geology Algorithms: Vectors and Tensors*. Cambridge, UK: University Press, Cambridge.

Ambrosius, B., Vigny, C., Chamot-Rooke, N., Le Pichon, X., Morgan, P., & Matheussen, S. (2001). Crustal motion and block behavior in SE-Asia from GPS measurements. *Earth and Planetary Science Letters*, 187(3-4), 239-244. https://doi.org/10.1016/S0012-821X(01)00298-9

An, A. R., Choi, S. H., Yu, Y., & Le, D-C. (2017). Petrogenesis of Late Cenozoic basaltic rocks from southern Vietnam. *Lithos*, 272-273, 192-204. https://doi.org/10.1016/j.lithos.2016.12.008

Anh, H. T. H., Choi, S. H., Yu, Y., & Pham, T. H. (2021). Geochemical constraints on the evolution of the lithospheric mantle beneath central and southern Vietnam. *Geosciences Journal*, 25(4), 433-451. https://doi.org/10.1007/s12303-020-0045-4

Anh, T. T., Long, T. V., & Nghiep, V. C. (2011). Geology and Earth Resources of Vietnam. In T. V. Tri, V. Khuc (Eds.), *Ministry of Natural Resources and Environment, General Department of Geology and Minerals of Vietnam* (pp. 645). Hanoi: Publishing House for Science and Technology.

Avouac, J. P., & Tapponnier, P. (1993). Kinematic model of active deformation in Central-Asia. *Geophysical Research Letters*, 20(10), 895-898. https://doi.org/10.1029/93GL00128

Bai, L., Iidaka, T., Kawakutsu, H., Morita, Y., & Dzung, N. Q. (2009). Upper mantle anisotropy beneath Indochina block and adjacent regions from shear-wave splitting analysis of Vietnam broadband seismograph array data. *Physics of the Earth and Planetary Interiors*, 176(176), 33-43. https://doi.org/10.1016/j.pepi.2009.03.008

Barckhausen, U., Engels, M., Franke, D., Ladage, S., & Pubellier, M. (2014). Evolution of the South China Sea: Revised ages for breakup and seafloor spreading. *Marine and Petroleum Geology*, 58, 599-611. https://doi.org/10.1016/j.marpetgeo.2014.02.022

Briais, A., Patriat, P., & Tapponnier, P. (1993). Updated interpretation of magnetic anomalies and seafloor spreading stages in the South China Sea: Implications for the Tertiary tectonics of SE Asia. *Journal of Geophysical Research*, 98(B4), 6299-6328. https://doi.org/10.1029/92JB02280

Burberry, C. M., Elkins, L. J., Hoang, N., & Richard, N. (2023). Faults in Southern Vietnam - implications for extrusion of Indochina, *Mendeley Data*, 2. 10.17632/h4v7srkpc2.2

Calais, E., Dong, L., Wang, M., Shen, Z., & Vergnolle, M. (2006). Continental deformation in Asia from a combined GPS solution. *Geophysical Research Letters*, 33(24), https://doi.org/10.1029/2006GL028433

546 Cardwell, R. K., & Isacks, B. L. (1978). Geometry of the subducted lithosphere beneath the Banda Sea in Eastern
547 Indonesia from seismicity and fault plane solutions. *Journal of Geophysical Research*, 83(B6), 2825-2838.
548 https://doi.org/10.1029/JB083iB06p02825
549 Carter, A., Roques, D., & Bristow, C. S. (2000). Denudation history of onshore Central Vietnam: constraints on the
550 Cenozoic evolution of the western margin of the South China Sea. *Tectonophysics*, 322(3-4), 265-277.
551 https://doi.org/10.1016/S0040-1951(00)00091-3
552 Chamot-Rooke, N., & Le Pichon, X. (1999). GPS determined eastward Sundaland motion with respect to Eurasia
553 confirmed by earthquake slip vectors at Sunda and Philippine trenches. *Earth and Planetary Science*
554 *Letters*, 173(4), 439-455. https://doi.org/10.1016/S0012-821X(99)00239-3
555 Chen, L., Hiu, J., Yang, D., Song, H., & Wang, Z. (2017). Kinematic models for the opening of the South China
556 Sea: an upwelling divergent flow origin. *Journal of Geodynamics*, 107, 20-33.
557 https://doi.org/10.1016/j.jog.2017.03.002
558 Chi, C. T., & Dorobek, S. L. (2004). Cretaceous palaeomagnetism of Indochina and surrounding regions: Cenozoic
559 tectonic implications. In J. Malpas, C. J. N Fletcher, J. R. Ali, J. C. Aitchison (Eds.), *Aspects of the*
560 *Tectonic Evolution of China* (pp. 273-287). London, Geological Society of London.
561 Chi, C. T., & Geissman, J. (2013). A review of the paleomagnetic results of Cretaceous rock formations from
562 Vietnam, Indochina and South China, their Cenozoic tectonic implications. *Journal of* Geodynamics, 69,
563 54-64. https://doi.org/10.1016/j.jog.2011.11.008
564 Chung, S-L., Cheng, H., Jahn, B., O-Reilly, S. Y., & Zhu, B. (1997). Major and trace element, and Sr-Nd isotope
565 constraints on the origin of Paleogene volcanism in South China prior to the South China Sea opening.
566 *Lithos*, 40, 203-220. https://doi.org/10.1016/S0024-4937(97)00028-5
567 Clift, P., Lee, G. H., Duc, N. A., Barckhausen, U., Van Long, H., & Zhen, S. (2008). Seismic reflection evidence for
568 a Dangerous Grounds miniplate: No extrusion origin for the South China Sea. *Tectonophysics*, 27(3),
569 https://doi.org/10.1079/2007TC002216
570 Cullen, A., Reemst, P., Henstra, G., Gozzard, S., & Ray, A. (2010). Rifting of the South China Sea: New
571 perspectives. *Petroleum Geoscience*, 16(3), 273-282. https://doi.org/10.1144/1354-079309-908
572 Cung, T. C., & Geissman, J. W. (2013). A review of the paleomagnetic data from Cretaceous to lower Tertiary rocks
573 from Vietnam, Indochina and South China, and their implications for Cenozoic tectonism in Vietnam and
574 adjacent areas. *Journal of Geodynamics*, 69, 54-64. https://doi.org/10.1144/1354-079309-908
575 Curray, J. C. (1989). The Sunda Arc: A model for oblique plate convergence. *Netherland Journal of Sea Research*,
576 24(2-3), 131-140. https://doi.org/10.1016/0077-7579(89)90144-0
577 Dewey, J. F., Taylor, T. R., & Monastero, F. C. (2008). Transtension in the Brittle Field: The Coso Region,
578 Southern California. *International Geology Review*, 50(3), 193-217. https://doi.org/10.2747/0020-
579 6814.50.3.193
580 Drury, S. A. (2004). Image Interpretation in Geology (3rd Ed). Cheltenham, UK: Routledge.
581 Eckert, A. & Connolly, P.T., 2007. Stress and Fluid-flow Interaction For the Coso Geothermal Field Derived From
582 3D Numerical Models. *In* Proceedings of the Geothermal Resources Council-Annual Meeting of the

583 Geothermal Resources Council, Renewable Baseload Energy: Geothermal Heat Pumps to Engineered
584 Reservoirs (Reno, NV), vol. 31, pp. 385 - 390, Elsevier B.V.
585 Ferrari, O. M., Hochard, C., & Stampfli, G. M. (2008). An alternative plate tectonic model for the Palaeozoic-Early
586 Mesozoic Palaeotethyan evolution of Southeast Asia (Northern Thailand–Burma). *Tectonophysics*, 451(1-
587 4), 346-365. https://doi.org/10.1016/j.tecto.2007.11.065
588 Fitch, T. J. (1972). Plate convergence, transcurrent faults, and internal deformation adjacent to Southeast Asia and
589 the Western Pacific. *Journal of Geophysical Research*, 77(23), 4432- 4460.
590 https://doi.org/10.1029/JB077i023p04432
591 Finzel, E. S., Flesch, L. M., & Ridgeway, K. D. (2011). Kinematics of a diffuse North American- Pacific-Bering
592 plate boundary in Alaska and western Canada. *Geology*, 39(9)0, 835-838. https://doi.org/10.1130/G32271.1
593 Flower, M., Hoang, N., & Tamaki, K. (1998). Mantle Extrusion' a Model for Dispersed Volcanism and DUPAL-like
594 Asthenosphere in East Asia and the Western Pacific. *American Geophysical Union*, 27, 67-88.
595 https://doi.org/10.1029/GD027p0067
596 Fyhn, M. B., Cuong, T. D., Hoang, B. H., Hovikoski, J., Olivarius, M., Tuan, N. Q., Tung, N. T., Huyen, N. T.,
597 Cuong, T. X., Nytoft, H. P., & Abatzis, I. (2018). Linking Paleogene Rifting and Inversion in the Northern
598 Song Hong and Beibuwan Basins, Vietnam, With Left- Lateral Motion on the Ailao Shan- Red River Shear
599 Zone. *Tectonics*, 37(8), 2559-2585. https://doi.org/10.1029/2018TC005090
600 Fyhn, M. B. W., Boldreel, L. O., & Nielsen, L. H. (2009a). Geological development of the Central and South
601 Vietnamese margin: Implication for the establishment of the South China Sea, Indochinese escape
602 tectonics, and Cenozoic volcanism. *Tectonophysics*, 478(3-4), 184-214.
603 https://doi.org/10.1016/j.tecto.2009.08.002
604 Fyhn, M. B. W., Nielsen, L. H., Boldreel, L. O., Thang, L. D., Bojesen-Koefoed, J., Petersen, H. I., Huyen, N. T.,
605 Duc, N. A., Dau, N. T., Mathiesen, A., Reid, I., Huong, D. T., Tuan, H. A., Hien, L. V., Nytoft, H. P., &
606 Abatzis, I. (2009b). Geological evolution, regional perspectives and hydrocarbon potential of the northwest
607 Phu Khanh Basin, offshore Central Vietnam. *Marine and Petroleum Geology*, 26(1), 1-24.
608 https://doi.org/10.1016/j.marpetgeo.2007.07.014
609 Fyhn, M. B. W., & Phach, P. V. (2015). Late Neogene structural inversion around the northern Gulf of Tonkin,
610 Vietnam: Effects from right-lateral displacement across the Red River fault zone. *Tectonics*, 34(2), 290-
611 312. https://doi.org/10.1002/2014TC003674
612 Geological and Mineral Resources Map of Vietnam, B'Lao Region, 1:200,000 scale. 1998. Hanoi, Vietnam:
613 Department of Geology and Minerals.
614 Geological and Mineral Resources Map of Vietnam, Gia Ray Region, 1:200,000 scale. 1998. Hanoi, Vietnam:
615 Department of Geology and Minerals.
616 Hall, R. (1996). Reconstructing Cenozoic SE Asia. In R. Hall & D. Blundell, (Eds.), *Tectonic Evolution of SE Asia*
617 (pp. 153-184). London: Geological Society of London Special Publication.

Hall, R. (2002). Cenozoic geological and plate tectonic evolution of SE Asia and the SW Pacific: computer-based reconstructions, model and animations. *Journal of Asian Earth Sciences*, 20(4), 353-431. https://doi.org/10.1016/S1367-9120(01)00069-4

Hall, R. (2012). Late Jurassic-Cenozoic reconstructions of the Indonesian region and the Indian Ocean. *Tectonophysics*, 570-571, 1-41. 10.1016/j.tecto.2012.04.021

Hamilton, W. (1979). Tectonics of the Indonesian region. *United States Geological Society Professional Pape*r, 1078, 345. https://doi.org/10.3133/pp1078

Hara, H., Tokiwa, T., Kurihara, T., Charoentitirat, T., Ngamnithiporn, A., Visetnat, K., Tominaga, K., Kamata, Y., & Ueno, K. (2018). Permian-Triassic back-arc basin development in response to Paleo-Tethys subduction, Sa Kaeo-Chanthaburi area in Southeastern Thailand. *Gondwana Research*, 64, 50-66. https://doi.org/10.1016/j.gr.2018.06.007

Hoang, N., & Flower, M. J. (1998). Petrogenesis of Cenozoic Basalts from Vietnam: Implication for Origins of a 'Diffuse Igneous Province. *Journal of Petrology*, 39(3), 369-95. https://doi.org/10.1093/petroj/39.3.369

Hoang, N., Flower, M. J., & Carlson, R. W. (1996). Major, trace element, and isotopic compositions of Vietnamese basalts: interaction of enriched mobile asthenosphere with the continental lithosphere. *Geochimica et Cosmochimica Acta*, 60, 4329-4351

Hoang, N., Martin F. J., Cung, T. C., Pham, T. X., Hoang, V. Q., & Tran, T. S. (2013). Collision-Induced Basalt Eruptions at Pleiku and Buon Me Thuot, South-Central Vietnam. *Journal of Geodynamics*, 69, 65-83. https://doi.org/10.1016/j.jog.2012.03.012

Hoang, N., Shinjo, R., Phuc, L. T., Anh, L. D., & Huong, T. T. (2019). Pleistocene basaltic volcanism in the Krong No are and vicinity, Dac Nong Province (Vietnam). *Journal of Asian Earth Sciences*, 181(1), 1367-9120. https://doi.org/10.1016/j.jseaes.2019.103903

Hu, P., Zhai, Q., Jahn, B., Wang, J., Lee, H., & Tang, S. (2015). Early Ordovician granites from the South Qiangtang terrane, northern Tibet: Implications for the early Paleozoic tectonic evolution along the Gondwanan proto-Tethyan margin. *Lithosphere*, 220, 318-338. https://doi.org/10.1016/j.lithos.2014.12.020

Huchon, P., Le Pichon, X., & Rangin, C., (1994a). Indochina Peninsula and the collision of India and Eurasia. *Geology*, 22(1), 27-30. https://doi.org/10.1130/0091-7613(1994)022<0027:IPATCO>2.3.CO;2

Hung, D. D., Tsutsumi, Y., Hieu, P. T., Minh, N. T., Minh, P., Dung, N. T., Hung, N. B., Komatsu, T., Hoang, N. & Kawaguchi, K., (2022). Van Canh Triassic granite in the Kontum Massif, central Vietnam: geochemistry, geochronology, and tectonic implications. *Journal of Asian Earth Sciences: X*, 7. https://doi.org/10.1016/j.jaesx.2021.100075

Hutchison, C. S. (1989). Geological Evolution of Southeast Asia 1st Ed, Clarendon, Oxford: Oxford University Press.

Jiang, W., Yu, J-H., Wang, X., Griffin, W. L., Pham, T. H., Nguyen, D. L., & Wang F. (2020). Early Paleozoic magmatism in northern Kontum Massif, Central Vietnam: Insights into tectonic evolution of the eastern Indochina Block. *Lithosphere*, 376-377. https://doi.org/10.1016/j.lithos.2020.105750

Jolivet, L., Claudio, F., Thorsten, B., Magdala, T., Pietro, S., & Pierre, B. (2018). Mantle Flow and Deforming Continents: From India-Asia Convergence to Pacific Subduction. *Tectonics*, 37(9), 2887-2914. https://doi.org/10.1029/2018TC005036

Jolivet, L., Faccenna, C., d'Agostino, N., Fournier, M., & Worrall, D. (1999). The kinematics of marginal basins, examples from the Tyrrhenian, Aegean and Japan Seas. In C. Mac Niocaill P. D. Ryan (Eds.), *Continental tectonics* (pp. 21-53). London: Geological Society. https://doi.org/10.1144/GSL.SP.1999.164.01.04

Kamvong, T., Khin, Z., Meffre, S., Maas, R., Stein, H., & Lai, C. K. (2014). Adakites in the Truong Son and Loei fold belts, Thailand and Laos: Genesis and implications for geodynamics and metallogeny. *Gondwana Research*, 26, 165-184. https://doi.org/10.1016/j.gr.2013.06.011

Kasatkin, S. A., Phach, P. V., Anh, L. D., & Golozubov, V. V. (2017). Cretaceous strike-slip dislocations in the Dalat Zone (Southeastern Vietnam). *Russian Journal of Pacific Geology*, 11(6), 408-420. https://doi.org/10.1134/S1819714017060033

Katz, M. B. (1993). The Kannack complex of the Vietnam Kontum massif of the Indochina block: an exotic fragment of Precambrian Gondwanaland? In R. H., Findlay, R., Unrug, M. R., Banks, J. J., Veevers, (Eds.), *Gondwana 8* (pp. 161-164). Rotterdam, Balkema.

Lacassin, R., Maluski, H., Leloup, P. H., Tapponnier, P., Hinthong, C., Siribhakdi, K., Chuaviroj, S., & Charoenravat, A. (1997). Tertiary diachronic extrusion and deformation of western Indochina, structural and $^{40}Ar/^{39}Ar$ evidence from NW, Thailand. *Journal of Geophysical Research*, 102, 10013-10037. https://doi.org/10.1029/96JB03831

Lan, C. Y., Chung, S. L., Van Long, T., Lo, C. H., Lee, T. Y., Mertzman, S. A., & Shen, J. (2003). Geochemical and Sr-Nd isotopic constraints from the Kontum massif, Central Vietnam on the crustal evolution of the Indochina block. *Precambrian Research*, 122(1-4), 7-27. https://doi.org/10.1016/S0301-9268(02)00205-X

Lee, T. Y., Lo, C. H., Chung, S. L., Chen, C. Y., Wang, P. L., Lin, W. P., Hoang, N., Chi, C. T., & Yem, N. T. (1998). $^{40}Ar/^{39}Ar$ Dating Result of Neogene Basalts in Vietnam and its Tectonic Implication. In M. F. J. Flower, T. Y. Lee (Eds.), *Mantle Dynamics and Plate Interactions in East Asia*, Washington, DC: American Geophysical Union.

Leloup, P. H., Arnaud, N., Lacassin, R., Kienast, J. R., Harrison, T. M., Phan Trong, T. T., Replumaz, A., & Tapponnier, P. (2001). New constraints on the structure, thermochronology and timing of the Ailao Shan-Red River shear zone, SE Asia. *Journal of Geophysical Research*, 106(B4), 6683-6732. https://doi.org/10.1029/2000JB900322

Leloup, P. H., Lacassin, R., Tapponnier, P., Schärer, U., Zhong, D., Liu, X., Zhang, L., Ji, S., & Trinh, P. T. (1995). The Ailao Shan-Red River shear zone (Yunnan, China), Tertiary transform boundary of Indochina. *Tectonophysics*, 251(1-4), 3-84. https://doi.org/10.1016/0040-1951(95)00070-4

Lepvrier, C., Maluski, H., Van Tich, V., Leyreloup, A., Thi, P. T., & Van Vuong, N. (2004). The Early Triassic Indosinian orogeny in Vietnam (Truong Son Belt and Kontum Massif); implications for the geodynamic evolution of Indochina. *Tectonophysics*, 393(1-4), 87-118. https://doi.org/10.1016/j.tecto.2004.07.030

690 Lepvrier, C., Maluski, H., Van Vuong, N., Rogues, D., Axente, V., & Rangin, C. (1997). Indosinian NW-trending
691 shear zones within the Truong Son belt (Vietnam) $^{40}Ar/^{39}Ar$ Triassic ages and Cretaceous to Cenozoic
692 overprints. *Tectonophysics*, 283(1), 105-127. https://doi.org/10.1016/S0040-1951(97)00151-0
693 Lepvrier, C., Van Vuong, N., Maluski, H., Thi, P. T., & Van Vu, T. (2008). Indosinian tectonics in Vietnam.
694 *Comptes Rendus Geoscience*, 340(2-3), 94-111. https://doi.org/10.1016/j.crte.2007.10.005
695 Li, C-F., Li, J., Ding, W., Franke, D., Yao, Y., Shi, H., Pang, X., Cao, Y., Lin, J., Kulhanek, D., Williams, T., Bao,
696 R., Briais, A., Brown, E. A., Chen, Y., Clift, P. D., Colwell, F.S., Dadd, K. A., Hernandez-Almeida, I.,
697 Huang, X-L., Hyun, S., Jiang, T., Koppers, A. A. P., Li, Q., Liu, C., Liu, Q., Liu, Z., Nagai, R. D., Peleo-
698 Alampay, A., Su, X., Sun, Z., Tejada, M. L. G., Trinh, H. S., Yeh, Y-C., Zhang, C., Zhang, F., Zhang, G-
699 L., & Zhao, X. (2015). Seismic stratigraphy of the central South China Sea basin and implications for
700 neotectonics. *Journal of Geophysical Research*, 120(3), 1377-1399. https://doi.org/10.1002/2014JB011686
701 Marrett, R. A., & Allmendinger, R. W. (1990). Kinematic analysis of fault-slip data. *Journal of Structural Geology*,
702 12(8), 973-986. https://doi.org/10.1016/0191-8141(90)90093-E
703 Matthews, S. J., Fraser, A. J., Lowe, S., Todd, S. P., & Peel, F. J. (1997). Structure, stratigraphy and petroleum
704 geology of the SE Nam Con Son Basin, offshore Vietnam. *Geological Society, London, Special*
705 *Publication*, 126, 89-106. https://doi.org/10.1144/GSL.SP.1997.126.01.07
706 McCaffrey, R. (1991). Slip vectors and stretching of the Sumatran fore arc. *Geology*, 19 (9), 881-884.
707 https://doi.org/10.1130/0091-7613(1991)019<0881:SVASOT>2.3.CO;2
708 Michel, G. W., Yu, Y. Q., Zhu, S. Y., Reigber, C., Becker, M., Reinhart, E., Simons, W., Ambrosius, B., Vigny, C.,
709 Chamot-Rooke, N., Le Pichon, X., Morgan, P., & Matheussen, S. (2001). Crustal motion and block
710 behavior in SE-Asia from GPS measurements. *Earth and Planetary Science Letters*, 187(3-4), 239-244.
711 https://doi.org/10.1016/S0012-821X(01)00298-9
712 Metcalfe, I. (2013a). Tectonic evolution of the Malay Peninsula. *Journal of Asian Earth Sciences*, 76, 195-213.
713 https://doi.org/10.1016/j.jseaes.2012.12.011
714 Metcalfe, I. (2013b). Gondwana dispersion and Asian accretion: Tectonic and paleogeographic evolution of eastern
715 Tethys. *Journal of Asian Earth Sciences*, 66, 1-33. https://doi.org/10.1016/j.jseaes.2012.12.020
716 Metcalfe, I. (2017). Tectonic evolution of Sundaland. *Bulletin of the Gological Society of Malaysia*, 63, 27-60.
717 https://doi.org/10.7186/bgsm63201702
718 Morley, C. K. (2002). A tectonic model for Tertiary evolution of strike-slip faults and rift basins in SE Asia.
719 *Tectonophysics*, 347(4), 189-215. https://doi.org/10.1016/S0040-1951(02)00061-6
720 Morley, C. K. (2007). Variations in Late Cenozoic-Recent strike slip and oblique-extensional geometries, within
721 Indochina: The influence of pre-existing fabrics. *Journal of Structural Geology*, 29(1), 36-58.
722 https://doi.org/10.1016/j.jsg.2006.07.003
723 Morley, C. K. (2012). Late Cretaceous-Early Palaeogene tectonic development of SE Asia. *Earth-Science Reviews*,
724 https://doi.org/115(1-2), 37-75. 10.1016/j.earscirev.2012.08.002

Morley, C. K. (2016). Major unconformities/termination of extension events and associated surfaces in the South China Seas: review and implications for tectonic development. *Journal of Asian Earth Sciences*, 120, 62-86. https://doi.org/10.1016/j.jseaes.2016.01.013

Nagy, E. A., Maluski, H., Lepvrier, C., Schärer, U., Thi, P. T., Leyreloup, A., & Tich, V. V. (2001). Geodynamic significance of the Kontum massif in Central Vietnam: composite $^{40}Ar/^{39}Ar$ and U–Pb ages from Paleozoic to Triassic. *Journal of Geology*, 109(6), 755-770. https://doi.org/10.1086/323193

Nam, T. N., Sano, Y., Terada, K., Toriumi, M., Van Quynh, P., & Dung, L. T. (2001). First SHRIMP U–Pb zircon dating of granulites from the Kontum massif (Vietnam) and tectonothermal implications. *Journal of Asian Earth Sciences*, 19(1-2), 77-84. https://doi.org/10.1016/S1367-9120(00)00015-8

Nam, T. N., Sano, Y., Terada, K., Toriumi, M., Van Quynh, P., & Dung, L. T. (2001). First SHRIMP U–Pb zircon dating of granulites from the Kontum massif (Vietnam) and tectonothermal implications. *Journal of Asian Earth Sciences*, 19(1-2), 77-84. https://doi.org/10.1016/S1367-9120(00)00015-8

Nguyen, H. P., Bui, C. Q., & Nguyen, D. X., (2012). Investigation of earthquake tsunami sources, capable of affecting Vietnamese coast. *Natural hazards*, *64*(1), 311–327. https://doi.org/ 10.1007/s11069-012-0240-3

Nguyen, V. V., & Luong, T. T. H. (2019). Cenozoic paleostress evolution in south central Vietnam: Implication for changing dynamics of faulting along the eastern Indochina continental margin. *Journal of Asian Earth Sciences*, 185, 104006. https://doi.org/10.1016/j.jseaes.2019.104006

Nielsen, L. H., Peterson, H. I., Thai, N. D., Duc N. A., Fyhn, M. B. W., Boldreel, L. O., Taun, H. A., Lindstrom, S., & Hien L. V. (2007). A Middle-Upper Miocene fluvial-lacustrine rift sequence in the Song Ba Rift, Vietnam: an analogue to oil-prone, small-scale continental rift basins. *Petroleum Geoscience*, 13(2), 145-168. https://doi.org/10.1144/1354-079307-748

Schmidt, W. J., Handschy, J. W., Hoang, B. H., Morley, C. K., Linh, D. V., Tung, N. T., & Tuan, N. Q. (2021). Structure and tectonics of a Late Jurassic, arcuate fold belt in the Ban Don Group, Southern Vietnam. *Tectonophysics*, 817. https://doi.org/10.1016/j.tecto.2021.229040

Sone, M., & Metcalfe, I. (2008). Parallel Tethyan sutures in Mainland Southeast Asia: new insights for Palaeo-Tethys closure and implications for the Indosinian orogeny. *Geosciences*, v. 340, 116-179. https://doi.10.1016/j.crte.2007.09.008

Sone, M., Metcalfe, I., & Chadumrong, P. (2012). The Chanthaburi terrane of southeastern Thailand: Stratigraphic confirmation as a disrupted segment of the Sukhothai Arc. *Journal of Asian Earth Sciences*, 61, 16-32. https://doi.10.1016/j.jseaes.2012.08.021

Pearce, M. & Dewey, J.F. (2008). Lithospheric-Scale Transtension between Vertical, Non-parallel, Planar Zone Boundaries. *International Geology Review*, 50(3), 325-342. https://doi.org/10.2747/0020-6814.50.3.325

Peltzer, G., & Saucier, F. (1996). Present-day kinematics of Asia derived from geologic fault rates. *Journal of Geophysical Research*, 101(B12), 27943-27956. https://doi.org/10.1029/96JB02698

Pubellier, M., & Morley, C. K. (2014). The basins of Sundaland (SE Asia): Evolution and boundary conditions. *Marine and Petroleum Geology*, 58, 555-578. https://doi.org/10.1016/j.marpetgeo.2013.11.019

761 Rangin, C., Huchon, P., Le Pichon, X., Bellon, H., Lepyrier, C., Roques, D., Hoe, H. D., & Ouynh, P. V., (1995).
762 Cenozoic deformation of central and south Vietnam. *Tectonophysics*, 251, 179-196.
763 https://doi.org/10.1016/0040-1951(95)00006-2
764 Redfield, T. F., Scholl, D. W., Fitzgerald, P. G., & Beck, M. E., Jr. (2007). Escape tectonics and the extrusion of
765 Alaska: Past, present and future. *Geology*, 35, 1039-1042. https://doi.org/10.1130/G23799A.1
766 Ridgeway, K. D., & Flesch, L. M. (2007). Cenozoic tectonic processes along the Southern Alaska convergent
767 margin. *Geology*, 35, 1055-1056. https://doi.org/10.1130/focus112007.1
768 Richter, B., & Fuller, M. (1996). Palaeomagnetism of the Sibumasu and Indochina blocks: Implications for the
769 extrusion tectonic model. In R. Hall, D. Blundell (Eds.), *Tectonic evolution of Southeast Asia*, London:
770 Geological Society Special Publications.
771 Roger, F., Maluski, H., Leyreloup, A., Lepvrier, C., & Phan, T. T. (2007). U-Pb dating of high temperature
772 metamorphic episodes in the Kon Tum Massif (Vietnam). *Journal of Asian Earth Sciences*, 30(3-4), 565-
773 572. https://doi.org/10.1016/j.jseaes.2007.01.005
774 Roques, D., Rangin, C., & Huchon, P. (2007). Geometry and sense of motion along the Vietnam continental margin:
775 onshore/offshore Da Nang area. *de la Societe Geologique de France*, 168(4), 413-422.
776 Savva, D., Meresse, F., Pubellier, M., Chamot-Rooke, N., Lavier, L., Wong Po, K., Franke, D., Steuer, S., Sapin, F.,
777 Auxietre, J. L., & Lamy, G. (2013). Seismic evidence of hyper-stretched crust and mantle exhumation
778 offshore Vietnam. *Tectonophysics*, 608, 72-83. https://doi.org/10.1016/j.tecto.2013.07.010
779 Searle, M. P., Yeh, M-W., Lin, T-H., & Chung, S-L. (2010). Structural constraints on the timing of left-lateral shear
780 along the Red River shear zone in the Ailao Shan and Diancang Shan Ranges, Yunnan, SW China.
781 *Geosphere*, 6, 316-338. https://doi.org/10.1130/GES00580.1
782 Simons, W. J. F., Socquet, A., Vigny, C., Ambrosius, B. A. C., Haji Abu, S., Promthon, C., Subarya, C., Saristo, D.
783 A., Matheussen, S., Morgan, P., & Spakman, W. (2007). A decade of GPS in Southeast Asia: Resolving
784 Sundaland motion and boundaries. *Journal of Geophysical Research*, 112**(**B6), 72-83.
785 https://doi.org/10.1029/2005JB003868
786 Steiger, R. H., & Jäger, E. (1977). Submission on geochronology: Convention on the use of decay constants in geo-
787 and cosmochronology. *Earth and Planetary Science Letters*, 36(3), 359-362. https://doi.org/10.1016/0012-
788 821X(77)90060-7
789 Taylor, B., & Hayes, D. E. (1983). Origin and history of the South China Basin. In D. E., Hayes (Eds.), *The Tectonic*
790 *and Geologic Evolution of Southeast Asia Seas and Islands* (pp. 25-56). Washington, DC: American
791 Geophysical Union. https://doi.org/10.1029/GM027p0023
792 Thuy, N. T. B., Satir, M. Siebel, W., Vennemann, T., Long, T.V. (2004). Geochemical and isotopic constraints on
793 the petrogenesis of granitoids from the Dalat zone, southern Vietnam. *Journal of Asian Earth Sciences*, 23,
794 467-482. https://doi.org/10.1016/j.jseaes.2003.06.001
795 Tri, T. V., & Khuc, V. (2011). Geology and earth resources of Vietnam. Hanoi, Vietnam: Publishing house for
796 Science and Technology.

Tingay, M., Morley, C., King, R., Hillis, R., Coblentz, D., & Hall, R. (2010). Present-day stress field of Southeast Asia. *Tectonophysics*, 482, 92-104. https://doi.org/10.1016/j.tecto.2009.06.019

Tran, D. T., Nguyen, T. Y., Duong, C. C., Vy, Q. H., Zuchiewicz, W., & Nguyen, V. N. (2013). Recent crustal movements of northern Vietnam from GPS data. *Journal of Geodynamics*, 69, 5-10.

Tapponnier, P., Peltzer, G., & Armijo, R. (1986). On the mechanics of the collision between India and Asia. *Geological Society, London, Special Publication*, 19, 113-157. https://doi.org/10.1144/GSL.SP.1986.019.01.0

Tapponnier, P., Peltzer, G., Le Dain, A. Y., Armijo, R., & Cobbold, P. (1982). Propagation extrusion tectonics in Asia: New insights from simple experiments with plasticine. *Geology*, 10, 611-616. https://doi.org/10.1130/0091-7613(1982)10<611:PETIAN>2.0.CO;2

Tingay, M., Morley, C., King, R., Hillis, R., Coblentz, D., & Hall, R. (2010). Present-day stress field of Southeast Asia. *Tectonophysics*, 482(1-4), 92-104. 10.1016/j.tecto.2009.06.019

Trinh, P. T., Van Liem, N., To, T. D., Van Huong, N., Hai, V. Q., Van Thom, B., Van Phong, T., Vinh, H. Q., Xuyen, N. Q., Thuan, N. V., & Tuc, N. D. (2015). Present day deformation in the east Vietnam Sea and surrounding regions. *Vietnam Journal of Marine Science and Technology*, 15(2), 105-118. https://doi.org/10.15625/1859-3097/15/2/6499

Tung, N. X., & Tri, T. V., (1992). Structural map of Vietnam (1:1,000,000). Hanoi: Geological Survey of Vietnam

Than, T. H., Hung, N. V., Quang, K. H. G., Ty, N. D., Quynh, N. H. (2003). Geological evolution and identification of hydrocarbon trapping types in the Phu Khanh Basin (in Vietnamese with English abstract). In H. Quy, N. H. Minh, (Eds.), *Proceedings of Conference on Vietnam Petroleum Institute. 25 years of Development and Achievements* (pp. 274-282) Hanoi, Vietnam.

Tran, T. H., Zaw, K., Halpin, J. A., Manaka, T., Meffre, S., Lai, C-K., Lee, L., Le, H. V., & Sang, D. (2014). The Tam Ky-Phuoc Son Shear Zone in central Vietnam: Tectonic and metallogenic implications. *Gondwana Research*, 26, 144-164. https://doi.org/10.1016/j.gr.2013.04.008

Usuki, T., Lan, C-Y., Yui, T-F., Iizuka, Y., Vu, T. V., Tran, T. A., Okamoto, K., Wooden, J. L., & Liou, J. G. (2009). Early Paleozoic medium-pressure metamorphism in Central Vietnam: evidence from SHRIMP U-Pb zircon ages. *Geoscience Journal*, 13, 245-256. https://doi.org/10.1007/s12303-009-0024-2

Phach, P. V., & Anh, L. D. (2018). Tectonic evolution of the southern part of Central Vietnam and the adjacent area. *Geodynamics & Tectonophysics*, 9(3), 801-825. doi:10.5800/GT-2018- 9-3-0372.

Van, D. C., Van, D. T., & Tran, V. T. (2001). Mafic and ultramafic formations in ophiolite belts of Vietnam. *Journal of Sciences of the Earth*, 23, 231-238.

Waight, T., Fynm, M. B. W., Thomsen, T. B., Tri, T. V., Nielsen, L. H., Abatzis, I., & Frei, D. (2021). Permian to Cretaceous granites and felsic volcanics from SW Vietnam and S Cambodia: Implications for tectonic development of Indochina. *Journal of Asian Earth Sciences*, 219, 1367-9120. https://doi.org/10.1016/j.jseaes.2021.104902

Wang, Y., Qian, X., Cawood, P.A., Liu, H., Feng, Q., Zhao, G., Zhang, Y., He, H., & Zhang, P. (2018). Closure of the East Paleotethyan Ocean and amalgamation of the Eastern Cimmerian and Southeast Asia continental fragragments. *Earth-Science Reviews*, 186, 195-230. https://doi.10.1016/j.earscirev.2017.09.013

Xu, C., Shi, H., Barnes, C. G., Zhou, Z. (2016). Tracing a late Mesozoic magmatic arc along the Southeast Asian margin from the granitoids drilled from the northern South China Sea. *Internaltional Geology Review*. 58(1), 71-94. https://doi.org/10.1080/00206814.2015.1056256

Yan, P., Deng, H., Liu, H., Zhang, Z., & Jiang, Y. (2006). The temporal and spatial distribution of volcanism in the South China Sea region. *Journal of Asian Earth Sciences*, 27, 647-659. 10.1016/j.jseaes.2005.06.005

Ye, Q., Mei, L., Shi, H, Camanni, G., Shu, Y, Wu, J., Yu, L., Deng, & Li, G. (2018). The Late Cretaceous tectonic evolution of the South China Sea area: An overview, and new perspectives from 3D seismic reflection data. *Earth-Science Reviews*, 187, 186-204. https://doi.org/10.1016/j.earscirev.2018.09.013

Zhou, D., Ru, K., & Chen, H. (1995). Kinematics of Cenozoic extension on the South China Sea continental margin and its implications for the tectonic evolution of the region. *Tectonophysics*, 251(1-4), 161-177. https://doi.org/10.1016/0040-1951(95)00018-6

Zhao, J., Xia, Y., Cannon, C. H., Kress., W. J., & Li, Q. (2016). Evolutionary diversification of alpine ginger reflects the early uplift of the Himalayan-Tibetan Plateau and rapid extrusion of Indochina. *Gondwana Research*, 32, 232-241. https://doi.org/10.1016/j.gr.2015.02.004

Zhu, M., Graham, S., & McHargue, T., (2009). The red river fault zone in the Yinggehai Basin, South China Sea. *Tectonophysics*, 476(3-4), 397-417. https://doi.org/10.1016/j.tecto.2009.06.015

Zhang, J. E., Xiao, W., Han, C., Mao, Q., Ao, S., Guo, Q., & Ma, C. (2011). A Devonian to Carboniferous intra-oceanic subduction system in Western Junggar, NW China. *Lithosphere*, 125, 592-606. https://doi.org/10.1016/j.lithos.2011.03.013

Zuchiewicz, W., Quốc Cu'ò'ng, N., Zasadni, J., & Yêm, N. T. (2013). Late Cenozoic tectonics of the Red River Fault Zone, Vietnam, in the light of geomorphic studies. *Journal of Geodynamic*s, 69, 11-30. https://doi.org/10.1016/j.jog.2011.10.008

FIGURE CAPTIONS

Figure 1. Map showing location of Indochina following India-Eurasia collision ~45 Ma (modified after Peltzer & Tapponnier, 1988; Tapponnier et al., 1990; Leloup et al., 1995; Morley et al., 2001; Morley, 2007; Zhang et al., 2011; Phach & Anh, 2018). This tectonic map of East and Southeast Asia shows red lines with sawtooth patterns indicating active subduction zones, while the thin red lines are extrusion-related sinistral strike-slip faults, including the Red River Fault Zone (RRFZ), the Wang Chao Fault Zone (WCFZ), and the Three Pagodas Shear Zone (TPSZ). Darker blue shades indicate the locations of marginal sea basins such as the East Vietnam/South China Sea (EVS/SCS). The Sundaland Block is outlined by the black dashed line and modified from Meltzner et al. (2017), and the study area is outlined by the yellow dashed line.

Figure 2. A simplified map of Vietnam where numbers indicate our field locations from this study. Volcanic plateaus (grey) with names were modified from Hoang et al. (2013), while Kasatkin et al. (2017) mapped the major strike-slip faults (red lines), which separate distinct lithosphere sectors. The large italic text surrounding the map is the name of each sector and the age of basement lithology. The thick black line shows the study area presented in

the subsequent figures. The names of the faults mapped by Kasatkin et al. (2017) are bolded and abbreviated next to the faults, which are VTCNF = Vung Tau Ca Na Fault, THCCF = Tuy Hoa Cu Chi Fault, SBF = Song Ba Fault, EVSZ = East Vietnam Shear Zone, PKSZ = Poko Shear Zone and TKPSSZ = Tam Ky Phuoc Son Shear Zone.

Figure 3. Contrasting fault maps for south-central Vietnam, after (a) Nguyen and Luong (2019) showing their interpretation of remotely sensed faults in the region; (b) Huchon et al. (1994a), with their interpretation of the Paleogene fault framework in the region; and (c) Rangin et al. (1995) with their contrasting interpretation of the dominant fault patterns in the area. The black box marks the location of the present study area. Grey shaded areas mark the boundaries of known basalt flows; the cross-cutting relationships between faults and basalt flows are unclear in all three interpretations.

Figure 4. DEM of Southern Vietnam overlain on a hillshade map to better highlight the Central Highlands region. Also shown are field locations for this study (stars, symbols as in Figure 2), mapped lineaments from this study (black lines), and major strike-slip faults (red lines) after Kasatkin et al. (2017) and this study.

Figure 5. Rose diagrams showing the orientations of lineaments (Figure 4) within the fault-bounded sectors (**a-f**), along with (**g-i**) a comparison with the orientations of mapped lineaments within the overall study area from previous work (indicated by the green border (Huchon et al., 1994; Rangin et al., 1994; Nguyen and Luong, 2019). All rose diagrams are in 5° bins, and the perimeter of the diagram is 5% of the data. (**j**) The key and red bars illustrate the orientations of the major block-bounding faults; EVTZ is the East Vietnam Transfer Zone, THCCF/VTCNF is the Tuy Hua Cu Chi and Vung Tau Ca Na faults respectively, which are broadly parallel to one another, SBF is the Song Ba fault, PKSZ is the Poko Shear Zone, and TKPSSZ is the Tam Ky Phuoc Son Shear Zone.

Figure 6. (a) Stereonets numbered 1-26 illustrate the orientations of measured fault planes for each field study location (Figure 2), with an example diagram shown as a legend in (b). The bold black lines in (a) group the local stereonets by lithospheric sector. Thick red lines in each stereonet indicate the main fault strands inferred from the average of our fault measurements for that field site, while blue and orange lines indicate sinistral and dextral faults, respectively. The grey-shaded lines are additional faults with field orientation measurements, but which lacked slip indicators.

Figure 7. Map of Vietnam with major volcanic centers in gray and the field area outlined in black, after Figure 2, and showing FaultKin™ stress regime solutions for field locations in this study; field locations are indicated using small numbers that correspond to the numbered locations in Figure 2. Colored borders indicate the age category, where cyan is “oldest,” yellow is “youngest,” and purple is “undefined,” as described in the text.

Figure 8. Combined steronet showing the calculated trend and plunge for the tensional axes derived from “oldest” and “youngest” cross-cutting slickensides, as well as “undefined” slickensides. Note the shift in trend and plunge values between the younger and older pairs of tensional axes, indicating a temporal change in principal stress directions.

Figure 9. Three locations showing cross-cutting strike- to oblique-slip and dip-slip lineations. (a) and (b) are from location 6, (c) and (d) are from Location 15, and (e) and (f) are from location 21. In each location, one photograph (images a, c, and e) is shown unaltered, and one photograph (images b, d, and f) has been artificially lightened and annotated to enhance the visibility of outcrop textures. All three locations show that the strike-slip to oblique-slip lineations cross-cut and are therefore younger than the dip-slip lineations.

Figure 10. Photographs illustrating examples of selected cross-cutting and field relationships for determining relative ages of faults in the study area; map locations as in Figure 2. (a) Fault surfaces in the Pliocene Soc Lu Formation at map location 14. The black dashed line shows the strike of the fault, and the red arrow shows the trend

and plunge of lineations on one fault plane. Other, similar fault plane lineations are illustrated with black arrows. (b) Neogene mafic intrusion (outline by the red dashed boundary) into a metasedimentary unit, at field location 21. (c) Positive flower structure identified within a Neogene basalt flow at map location 17. The red dashed lines illustrate the faulted surfaces.

Figure 11. Map of a subregion of the Da Lat study area showing age relationships between our mapped lineaments (Figure 2), and locations with age constraints (colored stars), all located within the Xuan Loc and Cu Chi Formations. Numbered dark purple stars mark field locations from this study (Figure 2); yellow stars mark locations with previously dated basalts (either from outcrop or cored sampling; Lee et al., 1998) that range in age from 2.42 ± 0.08 Ma in the south to 0.24 ± 0.06 Ma in the north part of the Xuan Loc Formation. Basalts at location 14 have also been previously dated by An et al. (2017) to be 4.3 ± 0.2 Ma. We measured a sample from location 11 and determined an age of 0.6 ± 0.004 Ma (see Supplementary Information). The geologic base map was modified after the Geological and Mineral Resources Map of Vietnam, Gia Ray Region (1998).

Figure 1.

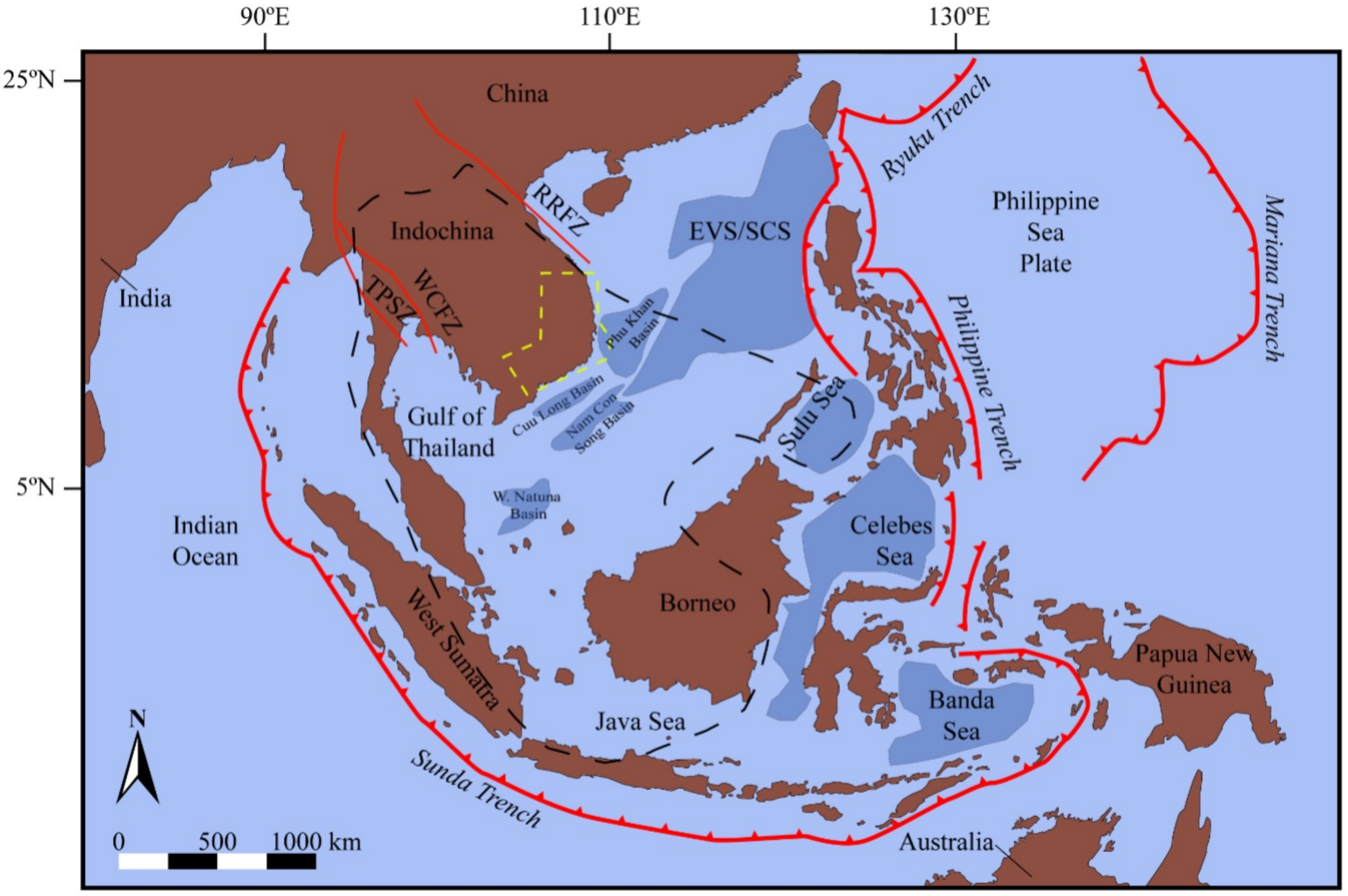
90ºE
110ºE
130ºE
25ºN
5ºN
China
India
Indochina
RRFZ
WCFZ
TPSZ
EVS/SCS
Phu Khan Basin
Cuu Long Basin
Nam Con Song Basin
Gulf of Thailand
W. Natuna Basin
Sulu Sea
Ryuku Trench
Philippine Sea Plate
Philippine Trench
Mariana Trench
Indian Ocean
West Sumatra
Borneo
Celebes Sea
Java Sea
Banda Sea
Papua New Guinea
Sunda Trench
Australia
N
0
500
1000 km

Figure 2.

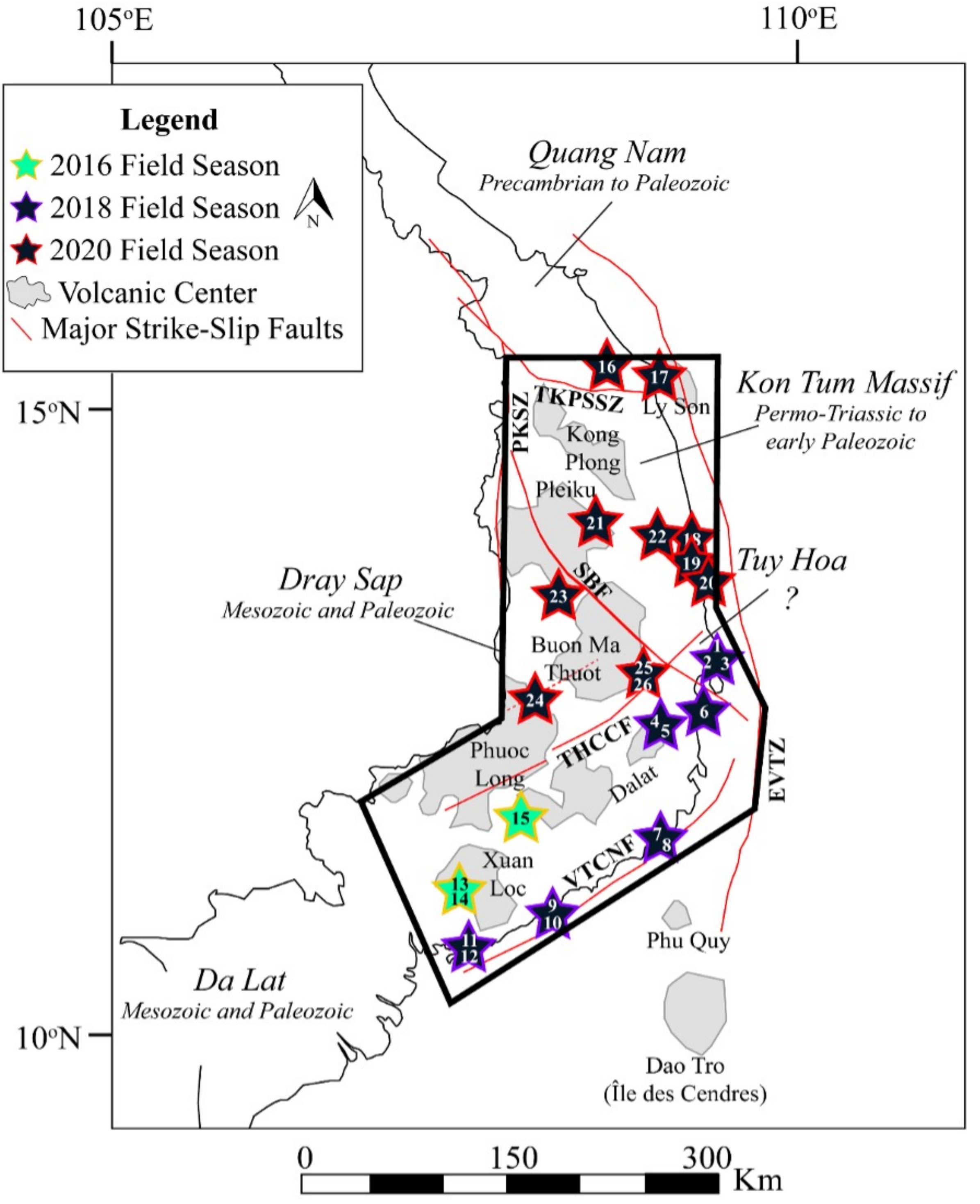
105°E
110°E
15°N
10°N
Legend
2016 Field Season
2018 Field Season
2020 Field Season
Volcanic Center
Major Strike-Slip Faults
N
Quang Nam
Precambrian to Paleozoic
Kon Tum Massif
Permo-Triassic to early Paleozoic
Dray Sap
Mesozoic and Paleozoic
Tuy Hoa
?
Da Lat
Mesozoic and Paleozoic
PKSZ
TKPSSZ
SBF
THCCF
VTCNF
EVTZ
Ly Son
Kong Plong
Pleiku
Buon Ma Thuot
Phuoc Long
Dalat
Xuan Loc
Phu Quy
Dao Tro
(Île des Cendres)
16
17
21
22
18
19
20
23
1
2
3
25
26
24
6
4
5
15
7
8
13
14
9
10
11
12
0
150
300
Km

Figure 3.

a

b

C

107°0'0"E
108°0'0"E
109°0'0"E
110°0'0"E
15°0'0"N
14°0'0"N
13°0'0"N
12°0'0"N
11°0'0"N
N
0 25 50 100 Kilometers

Legend

Boundaries of known basalt flows

Faults interpreted by Nguyen & Luong (a)

Faults interpreted by Huchon et al. (b)

Faults interpreted by Rangin et al. (c)

Figure 4.

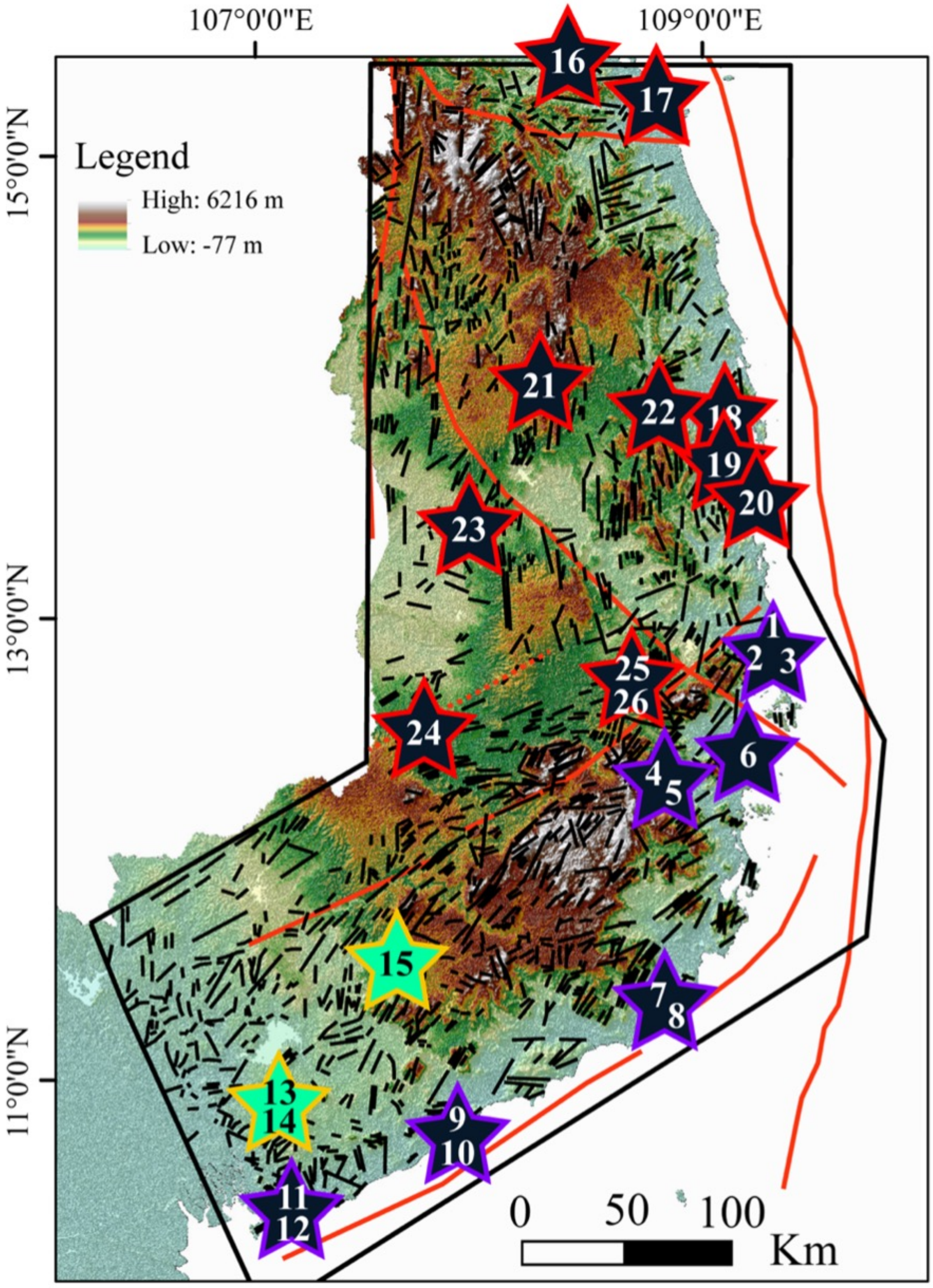
107°0'0"E
109°0'0"E
15°0'0"N
13°0'0"N
11°0'0"N
Legend
High: 6216 m
Low: -77 m
16
17
21
22
18
19
20
23
1
2
3
25
26
24
6
4
5
15
7
8
13
14
9
10
11
12
0
50
100
Km

Figure 5.

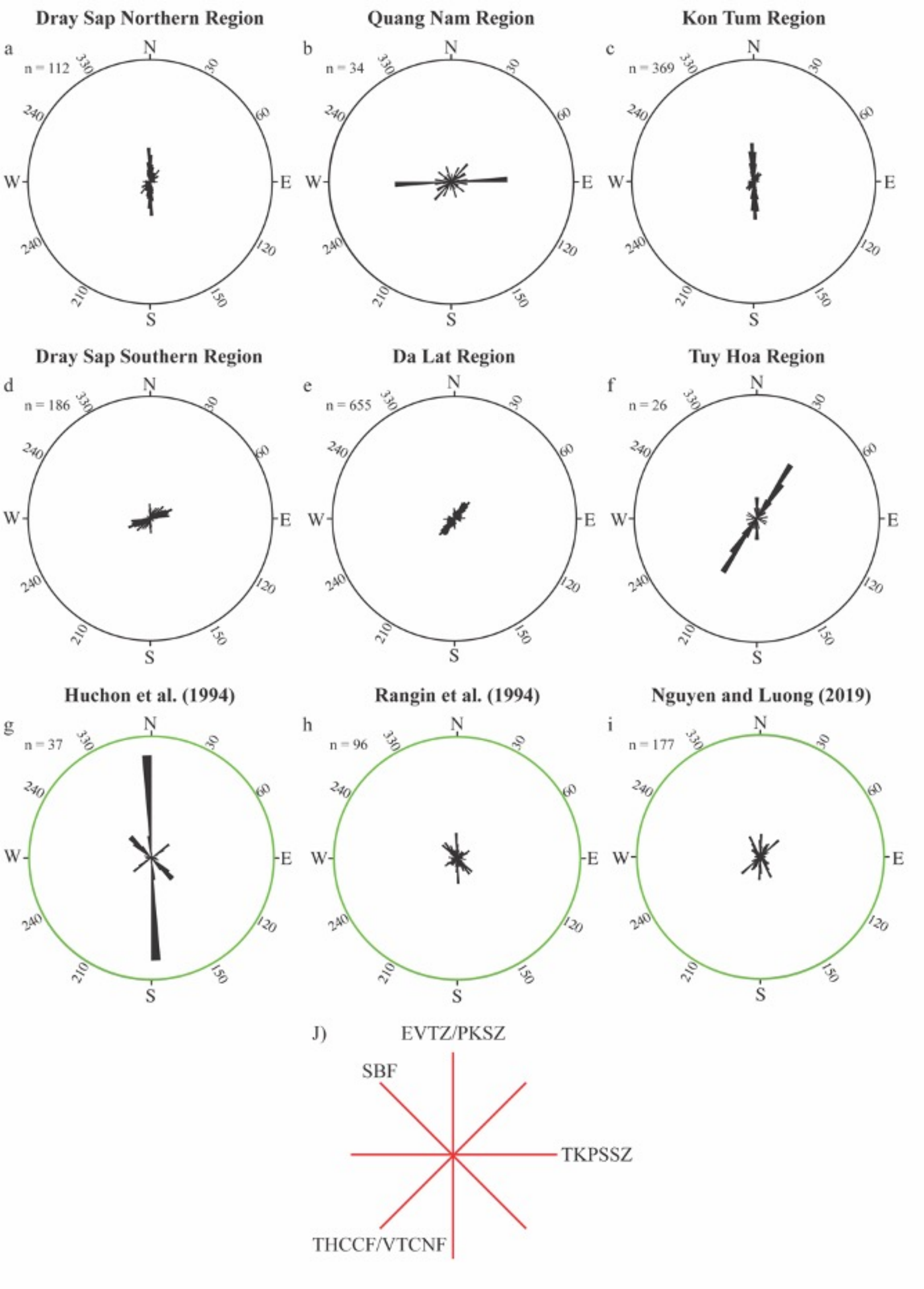
Dray Sap Northern Region
a
n = 112
Quang Nam Region
b
n = 34
Kon Tum Region
c
n = 369
Dray Sap Southern Region
d
n = 186
Da Lat Region
e
n = 655
Tuy Hoa Region
f
n = 26
Huchon et al. (1994)
g
n = 37
Rangin et al. (1994)
h
n = 96
Nguyen and Luong (2019)
i
n = 177
N
S
W
E
30
60
120
150
210
240
330
J)
EVTZ/PKSZ
SBF
TKPSSZ
THCCF/VTCNF

Figure 6a.

a

Tuy Hoa

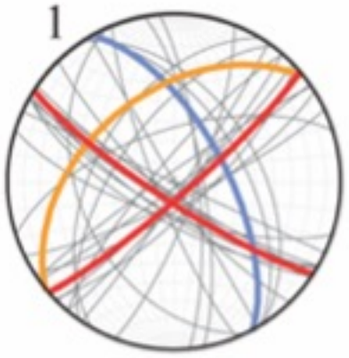
1

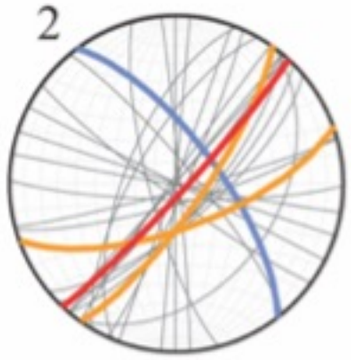
2

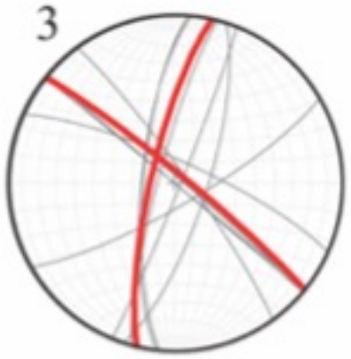
3

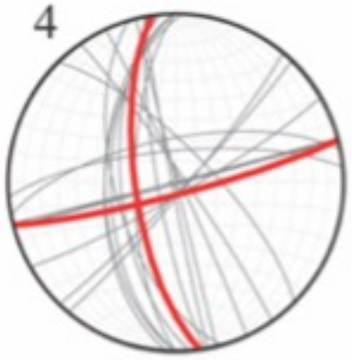
4

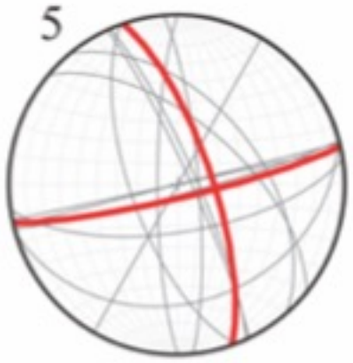
5

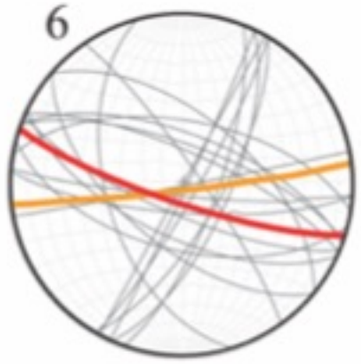
6

Da Lat

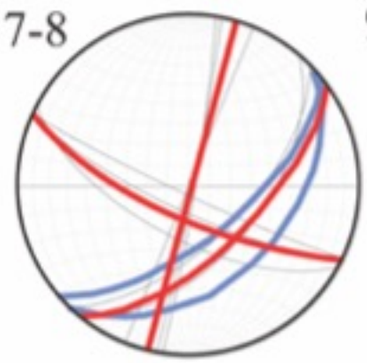
7-8

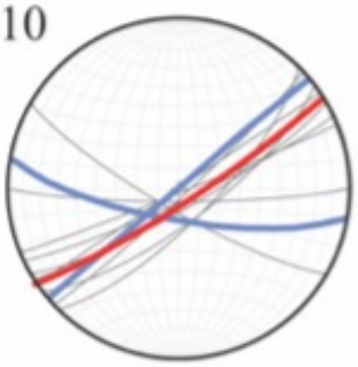
9-10

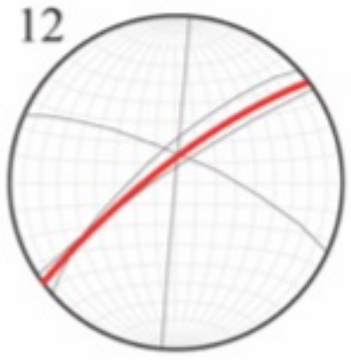
12

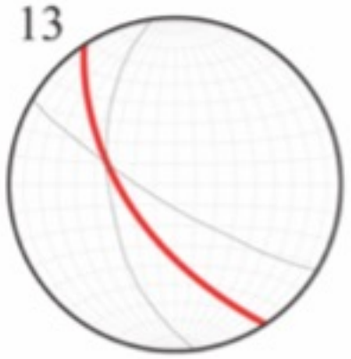
13

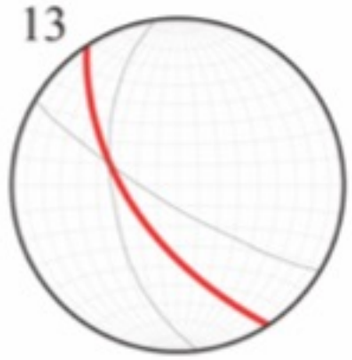
13

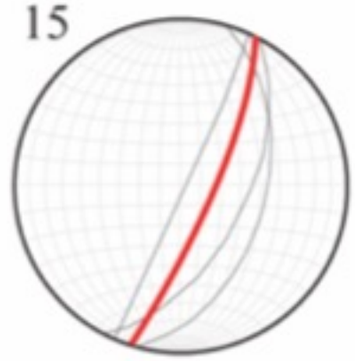
15

Quang Nam

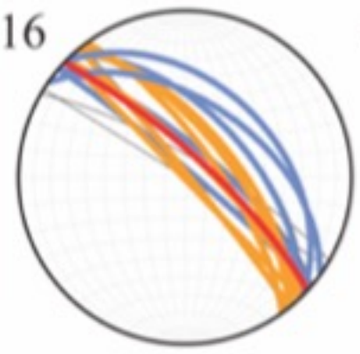
16

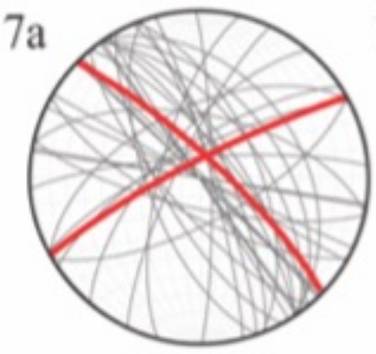
17a

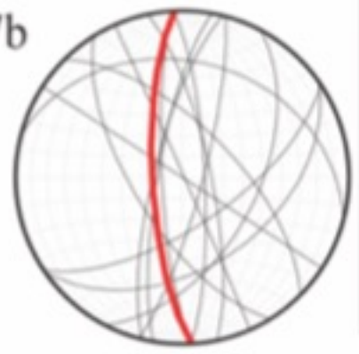
17b

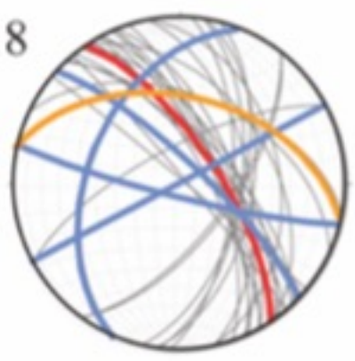
18

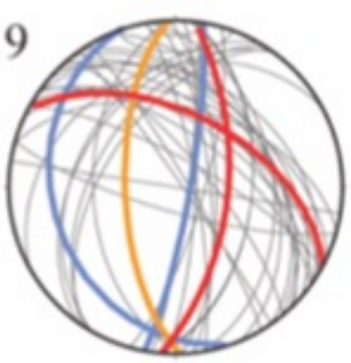
19

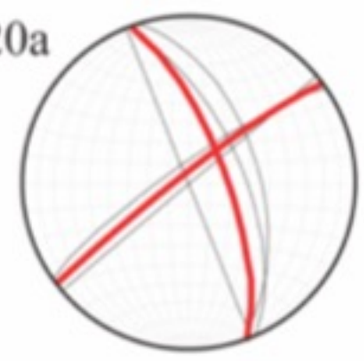
20a

Kon Tum

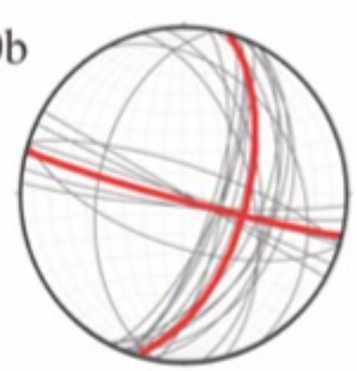
20b

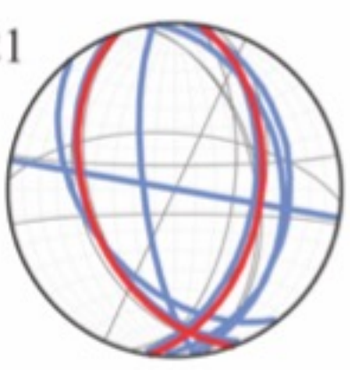
21

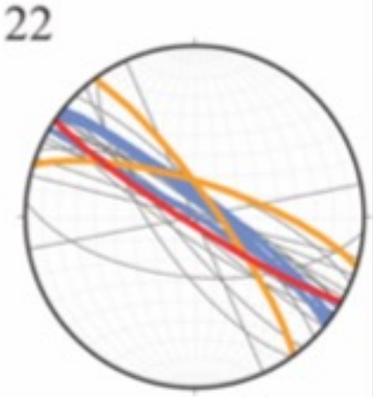
22

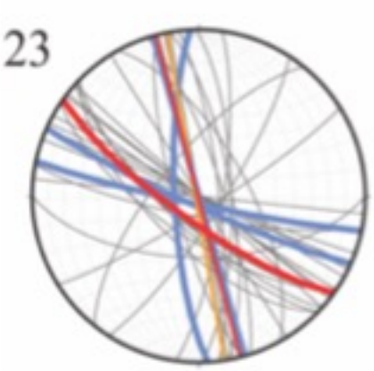
23

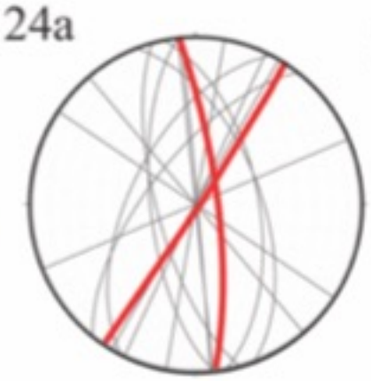
24a

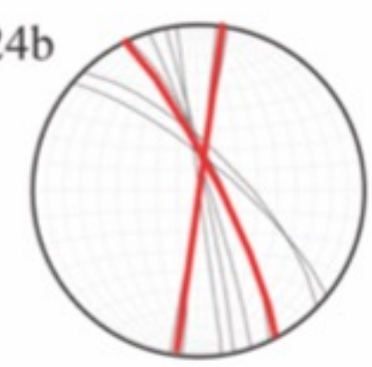
24b

Dray Sap

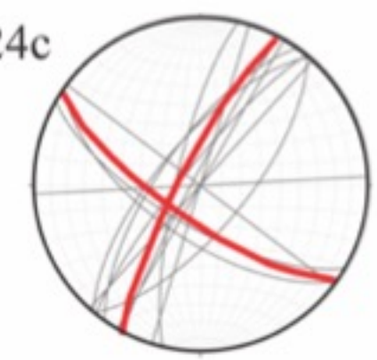
24c

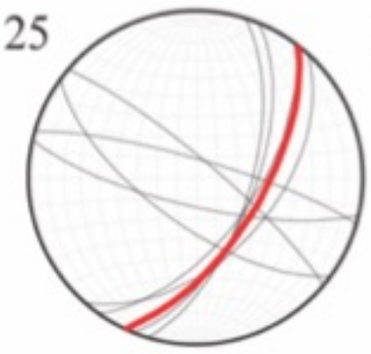
25

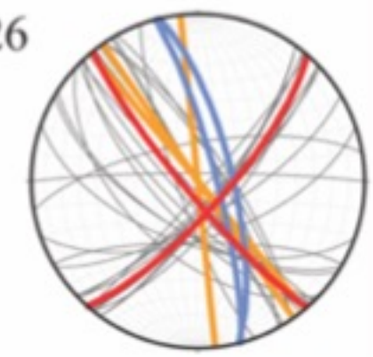
26

Figure 6b.

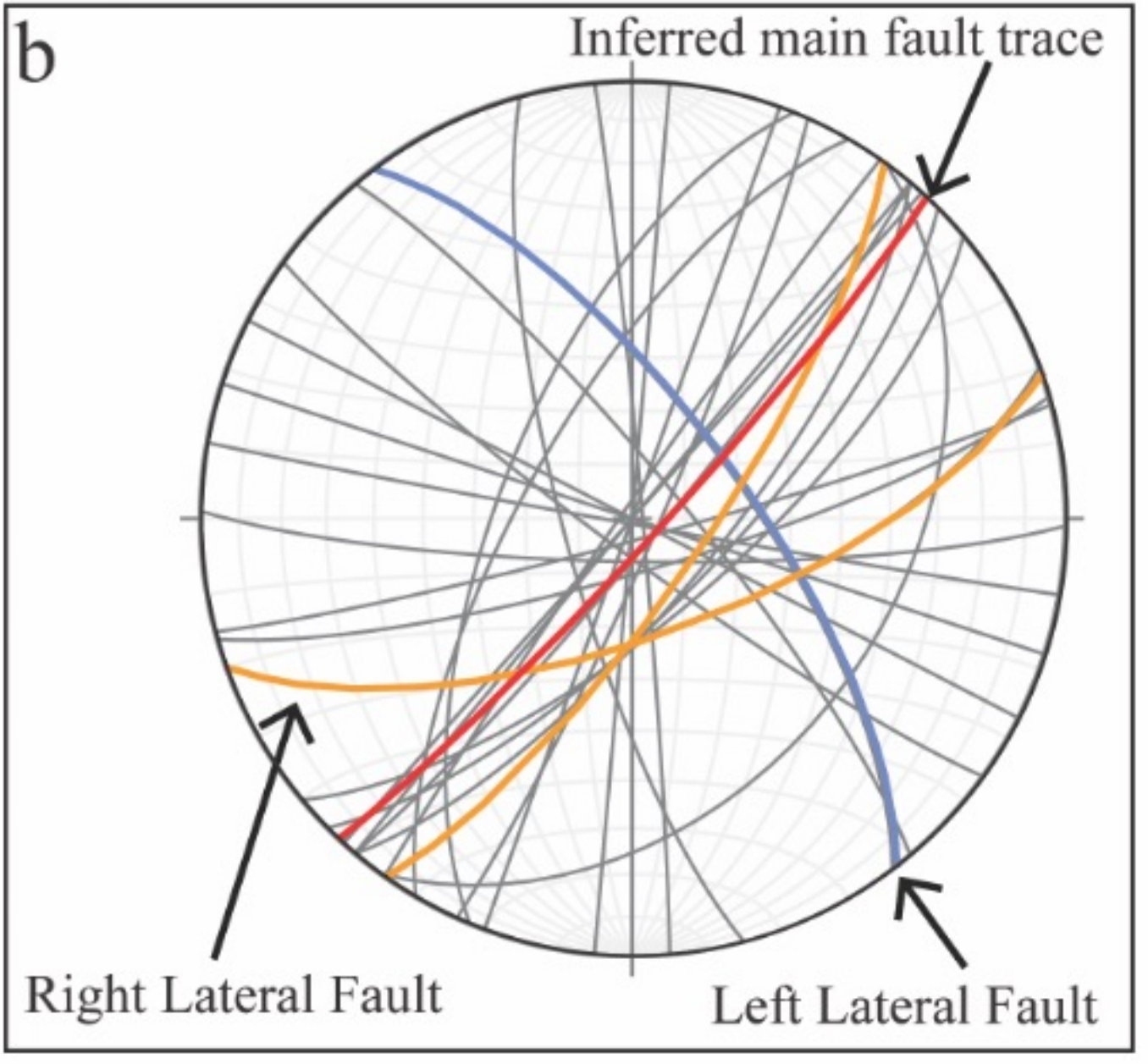
b
Inferred main fault trace
Right Lateral Fault
Left Lateral Fault

Figure 7.

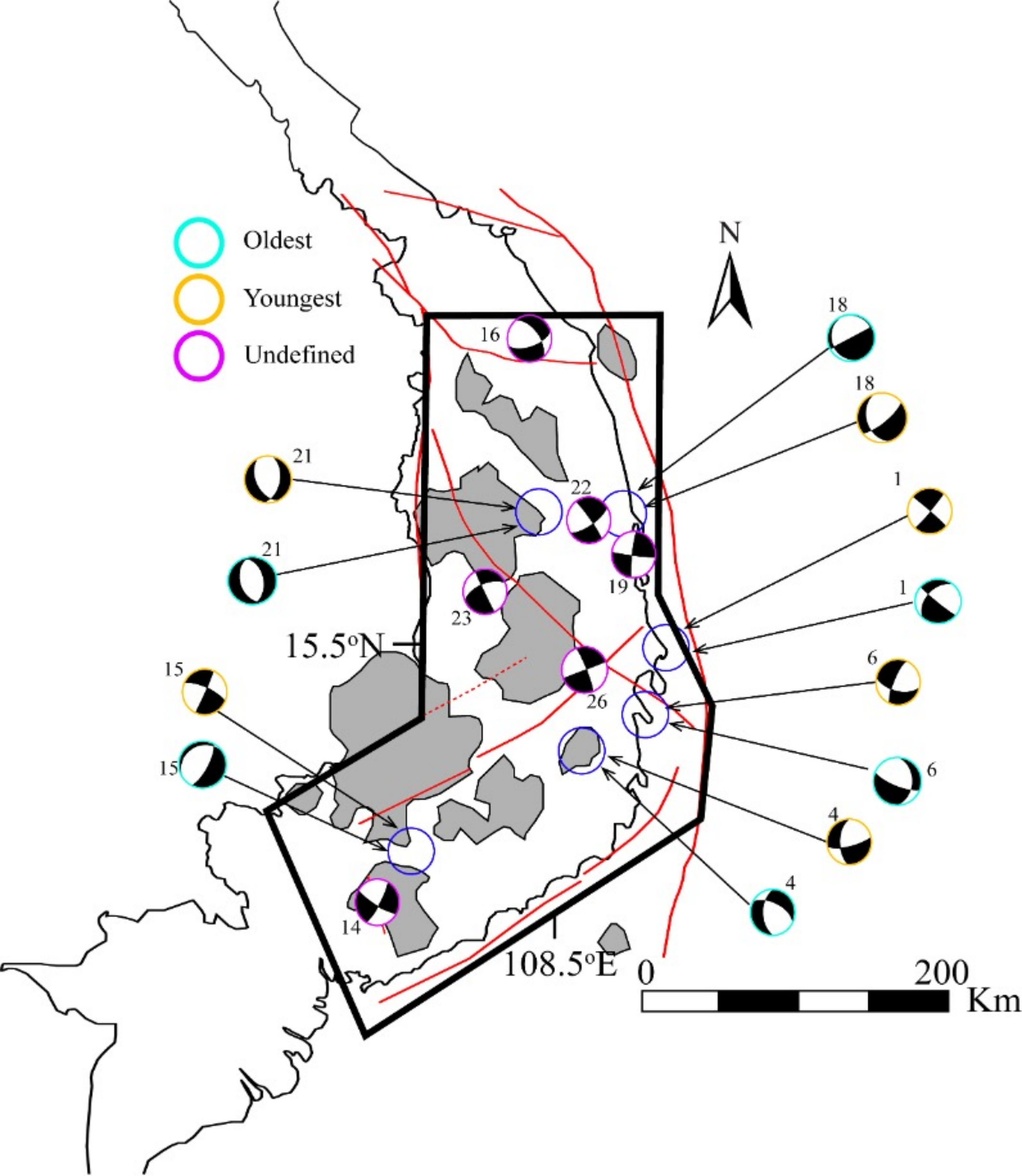
Oldest
Youngest
Undefined
N
16
18
18
21
22
1
21
19
1
23
15.5°N
15
26
6
15
6
4
14
4
108.5°E
0
200
Km

Figure 8.

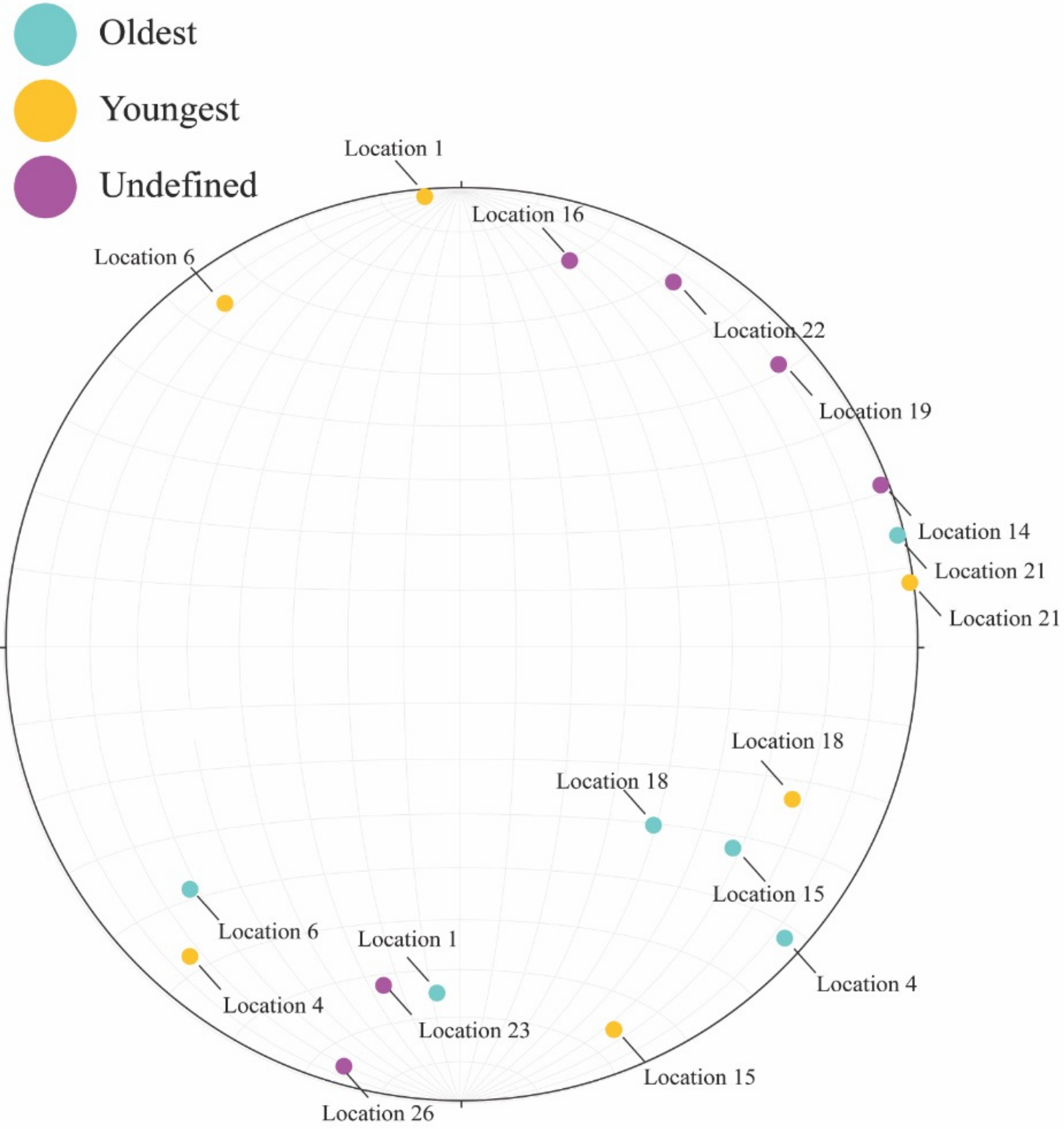
Oldest
Youngest
Undefined
Location 1
Location 16
Location 6
Location 22
Location 19
Location 14
Location 21
Location 21
Location 18
Location 18
Location 15
Location 6
Location 1
Location 4
Location 4
Location 23
Location 15
Location 26

Figure 9.

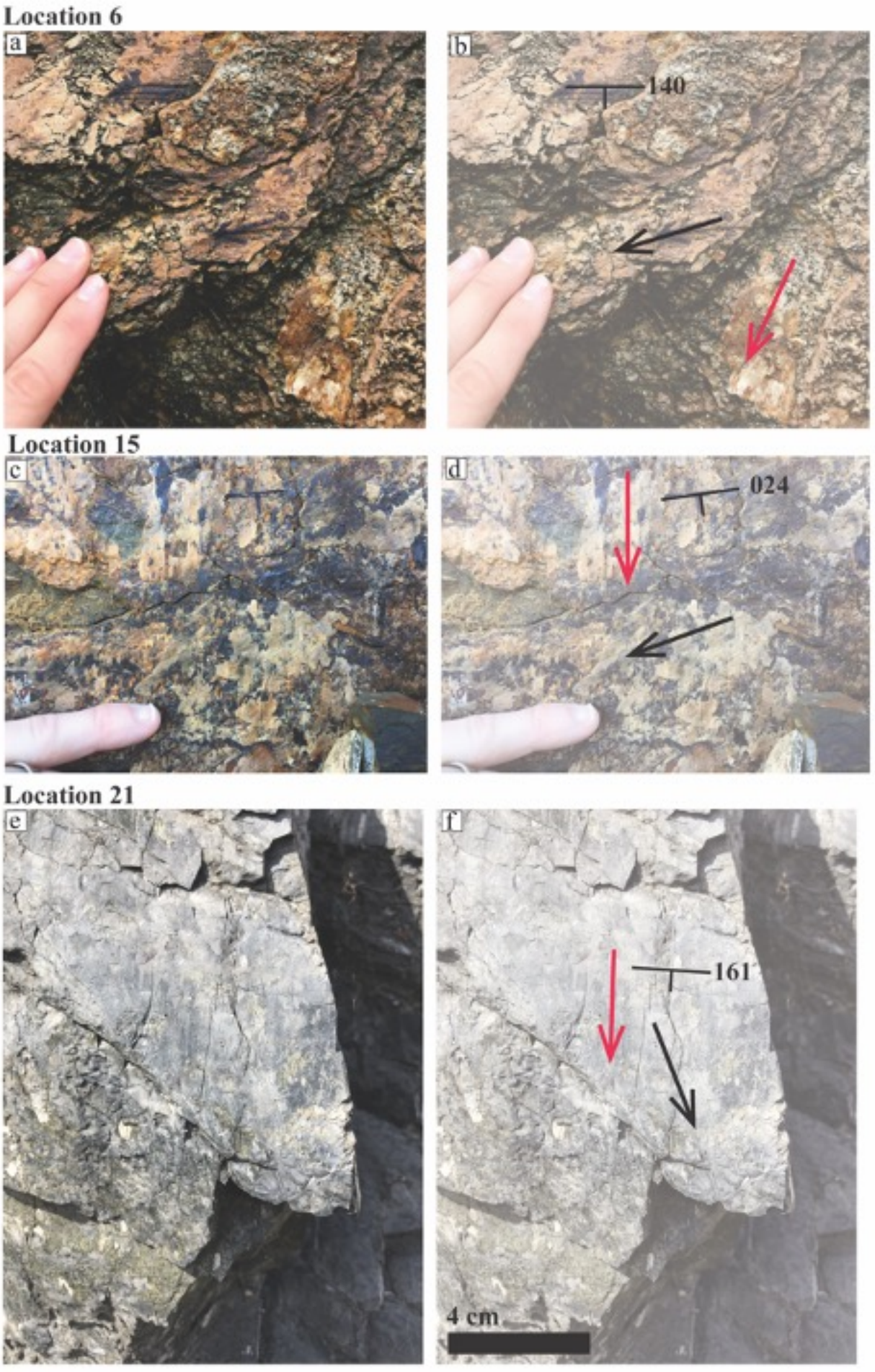
Location 6
a
b
140
Location 15
c
d
024
Location 21
e
f
161
4 cm

Figure 10.

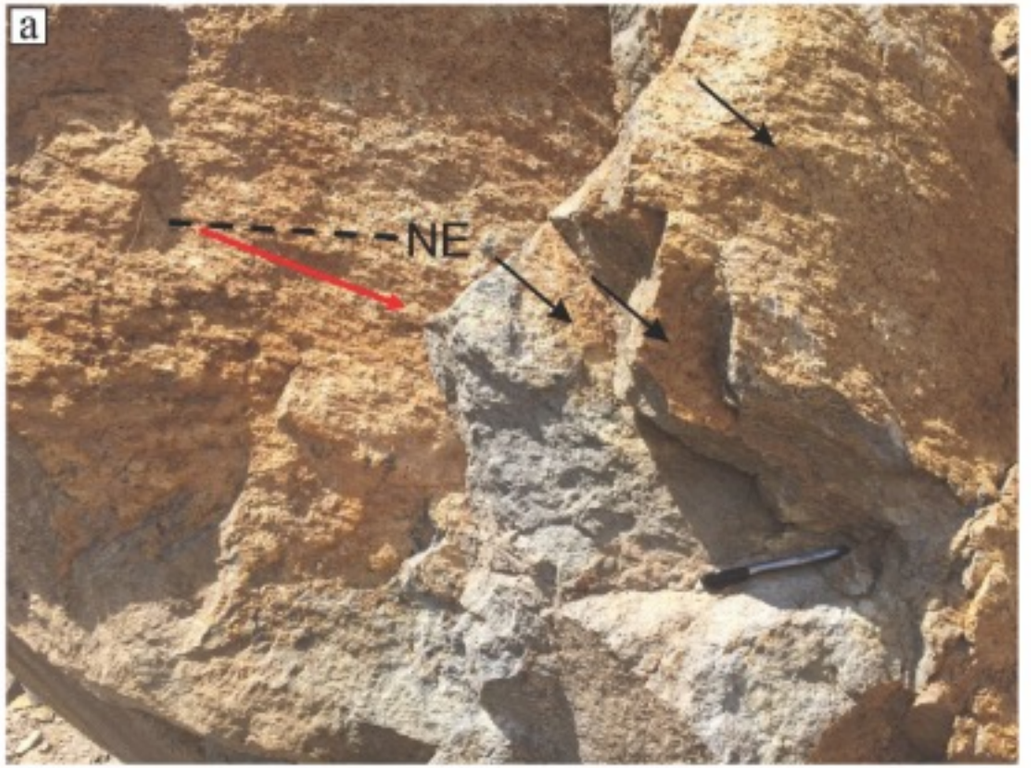
a
NE

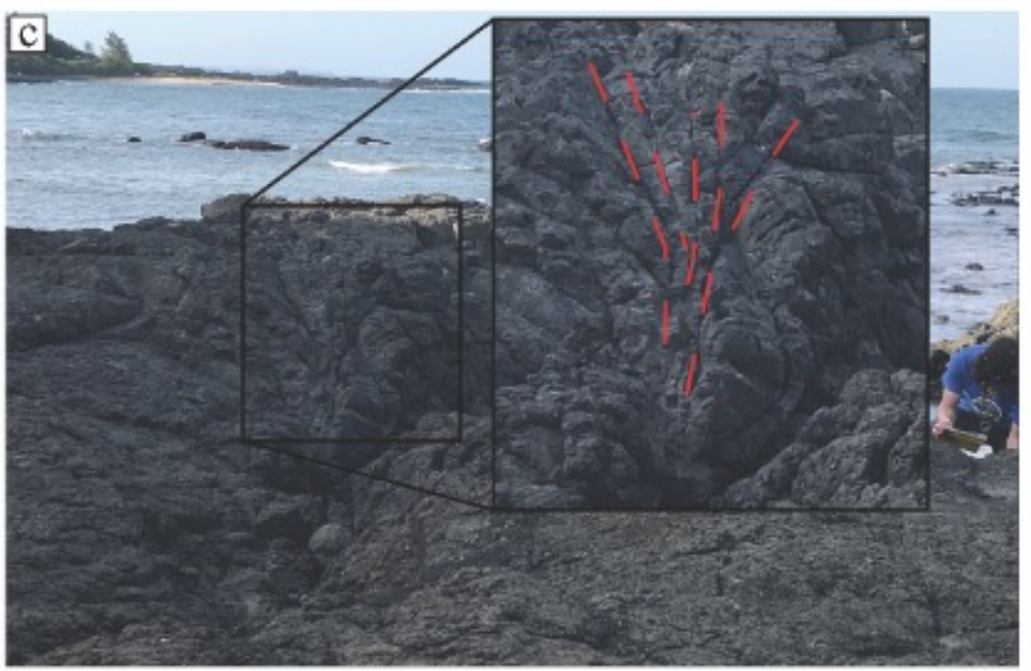
c


b

Figure 11.

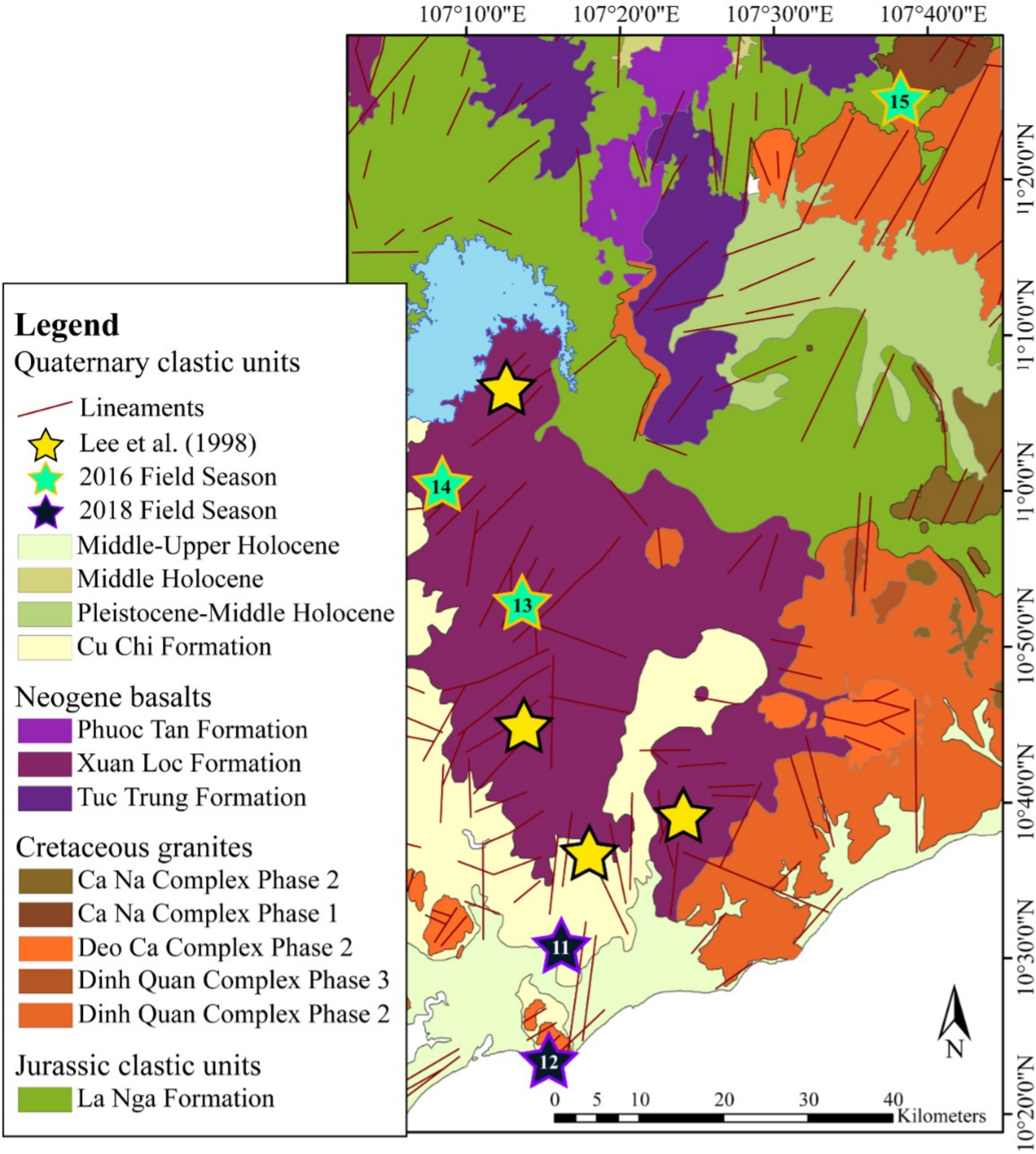
107°10'0"E
107°20'0"E
107°30'0"E
107°40'0"E
11°20'0"N
11°10'0"N
11°0'0"N
10°50'0"N
10°40'0"N
10°30'0"N
10°20'0"N
15
14
13
11
12
N
0 5 10 20 30 40
Kilometers
Legend
Quaternary clastic units
Lineaments
Lee et al. (1998)
2016 Field Season
2018 Field Season
Middle-Upper Holocene
Middle Holocene
Pleistocene-Middle Holocene
Cu Chi Formation
Neogene basalts
Phuoc Tan Formation
Xuan Loc Formation
Tuc Trung Formation
Cretaceous granites
Ca Na Complex Phase 2
Ca Na Complex Phase 1
Deo Ca Complex Phase 2
Dinh Quan Complex Phase 3
Dinh Quan Complex Phase 2
Jurassic clastic units
La Nga Formation